WHAT CAUSED THE GLACIAL/INTERGLACIAL ATMOSPHERIC pCO_2 CYCLES?

David Archer and Arne Winguth[1]
Department of the Geophysical Sciences
University of Chicago
Chicago, Illinois

David Lea
Department of Geological Sciences
University of California
Santa Barbara

Natalie Mahowald[2]
Department of Meteorology
University of Stockholm
Stockholm, Sweden

Abstract. Fifteen years after the discovery of major glacial/interglacial cycles in the CO_2 concentration of the atmosphere, it seems that all of the simple mechanisms for lowering pCO_2 have been eliminated. We use a model of ocean and sediment geochemistry, which includes new developments of iron limitation of biological production at the sea surface and anoxic diagenesis and its effect on $CaCO_3$ preservation in the sediments, to evaluate the current proposals for explaining the glacial/interglacial pCO_2 cycles within the context of the ocean carbon cycle. After equilibration with $CaCO_3$ the model is unable to generate glacial pCO_2 by increasing ocean NO_3^- but predicts that a doubling of ocean H_4SiO_4 might suffice. However, the model is unable to generate a doubling of ocean H_4SiO_4 by any reasonable changes in SiO_2 weathering or production. Our conclusions force us to challenge one or more of the assumptions at the foundations of chemical oceanography. We can abandon the stability of the "Redfield ratio" of nitrogen to phosphorus in living marine phytoplankton and the ultimate limitation of marine photosynthesis by phosphorus. We can challenge the idea that the pH of the deep ocean is held relatively invariant by equilibrium with $CaCO_3$. A third possibility, which challenges physical oceanographers, is that diapycnal mixing in ocean circulation models exceeds the rate of mixing in the real ocean, diminishing the model pCO_2 sensitivity to biological carbon uptake.

1. INTRODUCTION

Bubbles of ancient air trapped in Antarctic ice reveal that the pCO_2 of the glacial atmosphere was 80–90 μatm lower than the preanthropogenic interglacial value of 280 μatm. Radiative forcing from CO_2 accounts for maybe half of the glacial/interglacial climate change [*Manabe and Broccoli*, 1985; *Webb et al*., 1997]. Subsequent data show a tight repeatable correlation between pCO_2 and the ice volume and temperature records from the last two glacial/interglacial cycles (Figure 1). However, in spite of the clear importance of pCO_2 as an amplifier or even a primary driver of the glacial cycles, and the additional motivation provided by the threat of future climate change, we remain ignorant of the mechanisms responsible for the glacial/interglacial CO_2 cycles.

The glacial cycles are marked by the advances and retreats of the major ice sheets and are documented by the isotopic composition of oxygen in seawater as recorded in $CaCO_3$. The oceans become enriched in the heavier isotope ^{18}O as the lighter ^{16}O is selectively sequestered in glacial ice. These advances and retreats correlate with variations in the Earth's orbit. Integrated over the surface of the Earth and over the course of a year, the total energy received from the Sun is relatively insensitive to these orbital variations, but the distribution of the solar energy varies significantly both latitudinally and seasonally. In particular, it appears that summer in the Northern Hemisphere is the sweet spot for climate in the current continental configuration [*Milankovitch*, 1930; *Hays et al*., 1976]. The Northern Hemisphere is where most of the ice sheets form, and summer is when the fate of winter ice is decided.

Three orbital cycles combine to modulate the Northern Hemisphere solar heating. The axis of rotation of the Earth precesses like a wobbling top, changing the location of Northern Hemisphere summer around the eccentric orbit of the Earth. This "precessional" cycle contains spectral energy at frequencies of 19 and 23 kyr. The rotational axis of the Earth is tilted relative to the plane of the orbit, and this angle (called the obliquity) varies between 22° and 25°, in cycles of 41 kyr. Third, the eccentricity of the orbit itself undergoes minima and maxima, modulating the impact of the precession cycles on supercycle timescales of 100 and 400 kyr.

The ice age cycles underwent a midlife transition

[1] Now at Department of Atmospheric and Oceanic Sciences, University of Wisconsin-Madison.

[2] Now at Donald Bren School of Environmental Science and Management, University of California, Santa Barbara.

Reviews of Geophysics, 38, 2 / *May 2000*
pages 159–189
8755-1209/00/1999RG000066*$15.00*
Paper number 1999RG000066

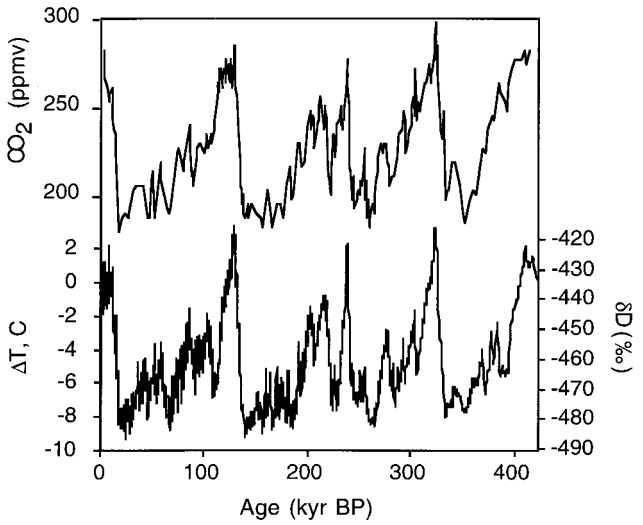

Figure 1. The pCO_2 [*Petit et al.*, 1999] and deuterium-based local temperature from the Vostok ice core.

about 800 kyr ago. Before this time the amplitude of the 20-, 40-, and 100-kyr cycles in glaciation as recorded by ^{18}O were in rough proportion to the Northern Hemisphere solar heat flux forcing as calculated from orbital theory. Beginning at 800 kyr B.P., the 100-kyr cycles grew stronger than their orbital forcing would seem to justify [*Imbrie et al.*, 1992, 1993]. To explain this apparent "low-frequency amplification," climate scientists are looking for components of the climate system which respond slowly to external forcing and thereby maintain a long memory, for example, the carbonate system of the ocean, the growth of continental ice sheets, or isostatic rebound of continental landmass following accumulation or removal of an ice sheet [*Imbrie et al.*, 1993].

We are still unsure whether CO_2 is a primary driver or a secondary amplifier of the glacial cycles. The Milankovitch orbital theory for the glacial cycles would seem to imply the latter, because there is a clear physical link between Northern Hemisphere summer heating and ice sheets but no easy link from orbital variations to pCO_2. However, in the last two glacial terminations, the pCO_2 rise clearly precedes the ^{18}O of the atmosphere (an indicator of melted ice sheets) by several thousand years [*Sowers and Bender*, 1995; *Broecker and Henderson*, 1998], implying that pCO_2 is a primary driver (Figure 2). Alternatively, pCO_2 could be driven by changes in meteorological forcing, such as dust delivery of trace metals to the ocean surface, resulting in an acausal correlation between Northern Hemisphere summer insolation and ice volume.

Most of the carbon on Earth is incorporated into $CaCO_3$ rocks, but this carbon pool turns over too slowly to account for pCO_2 changes over the glacial cycles [*Berner et al.*, 1983]. Carbon in the terrestrial biosphere is available on shorter time frames, but the terrestrial biosphere and soil carbon reservoirs would have to approximately double in size to deplete pCO_2 by 80 μatm. Instead, the $\delta^{13}C$ from deep-sea $CaCO_3$, more ^{12}C rich during glacial time, tells us that if anything, the terrestrial biosphere released carbon during glacial time [*Shackleton*, 1977], the wrong direction to explain lower glacial pCO_2. The only remaining candidate driver for the atmospheric CO_2 change is the ocean, which contains enough carbon to absorb the atmospheric decrease

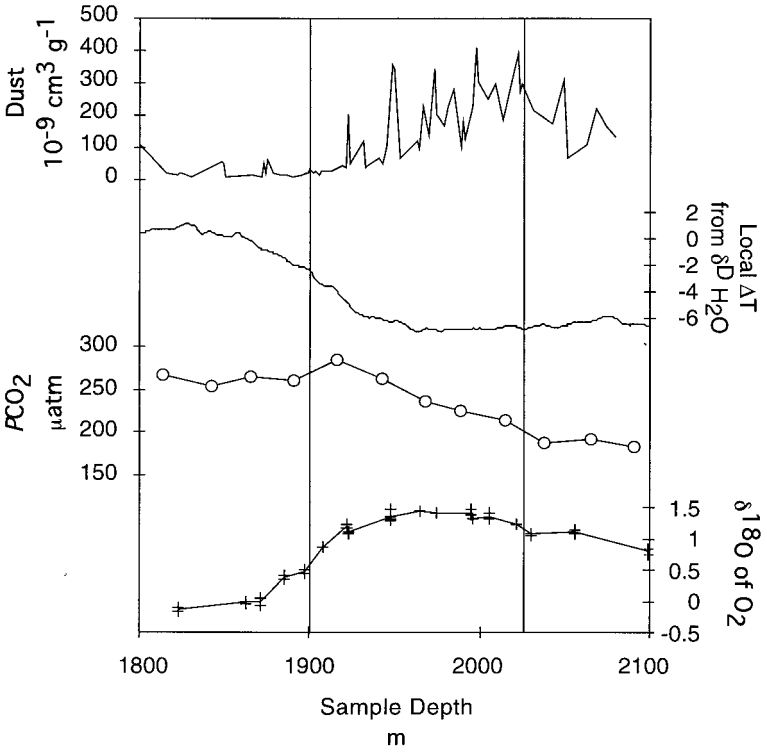

Figure 2. The sequence of events associated with termination II, following *Broecker and Henderson* [1998]. Total time span is about 28,000 years. Dust is from *Lorius et al.* [1985], pCO_2 is from *Petit et al.* [1999], and $\delta^{18}O$ of atmospheric oxygen is from *Sowers et al.* [1991], plotted against sample depth (as usual in geological records, older is deeper). The pCO_2 and $\delta^{18}O_2$ have been offset 40 m because gases in snowpack are free to exchange with the atmosphere until bubble close-off, which offsets the ages of gases and ice. The pCO_2 increase begins (right-hand vertical line, 134 kyr, from the *Lorius et al.* [1985] timescale) before the $\delta^{18}O$ of atmospheric O_2, reflecting ice volume (left-hand vertical line, ~158 kyr, from *Lorius et al.* [1985]).

and can change on the 1- to 10-kyr timescales recorded in the ice cores.

Ocean participation in the pCO_2 cycles in the atmosphere is documented by cycles of $CaCO_3$ deposition in the deep sea, marked by Atlantic to Pacific shifts in $CaCO_3$ burial [*Berger*, 1973; *Farrell and Prell*, 1989] and by $CaCO_3$ preservation anomalies on deglaciations and dissolution anomalies on glaciations [*Peterson and Prell*, 1985]. In some parts of the ocean the CO_2 concentration at the sea surface is supersaturated with respect to the pCO_2 of the atmosphere, and other parts are undersaturated [*Takahashi et al*., 1997], but the atmosphere as a whole represents an average of the surface water equilibrium gas phase chemistry [*Broecker and Peng*, 1982]. (At the present day, the large-scale equilibrium between the ocean and the atmosphere has been perturbed by the rapid increase in atmospheric pCO_2 caused by fossil fuel combustion.) Because CO_2 is more soluble in colder water, colder sea surface temperatures could lower pCO_2. However, the magnitude of the glacial cooling can account for only a small fraction of the observed pCO_2 drawdown.

The first proposed mechanisms to lower glacial pCO_2 were to increase the rate of biological productivity in surface waters of the ocean, exporting carbon from the surface ocean to the deep sea in the form of sinking particles. Either an increase in the ocean inventory of nutrients (PO_4^{3-} and NO_3^-), or a change in the ratio of nutrient to C in phytoplankton, could have stimulated the ocean's "biological pump" in this way [*Broecker and Peng*, 1982; *McElroy*, 1983; *Broecker and Henderson*, 1998]. Shortly thereafter, simple box models of the ocean carbon cycle showed that the pCO_2 of the atmosphere is extremely sensitive to the biological pump in high latitudes and insensitive to low-latitude forcing [*Knox and McElroy*, 1984; *Sarmiento and Toggweiler*, 1984; *Siegenthaler and Wenk*, 1984]. The observation that iron availability limits phytoplankton growth in remote parts of the ocean such as the Southern Ocean [*Martin and Fitzwater*, 1988] provided a mechanism by which the high-latitude biological pump could have intensified in a dustier [*Peteet et al*., 1990], more iron-rich glacial climate. A current form of this idea is for glacial dust to stimulate the rate of nitrogen fixation [*Falkowski*, 1997; *Broecker and Henderson*, 1998], increasing the ocean pool of NO_3^-.

A second class of mechanisms to lower glacial pCO_2 is to change the pH of the whole ocean, converting seawater CO_2 into HCO_3^- and $CO_3^=$, which are unable to evaporate into the atmosphere. The pH of the ocean is controlled by a mechanism known as $CaCO_3$ compensation; any imbalance between the influx of dissolved $CaCO_3$ from chemical weathering on land and the removal of $CaCO_3$ by burial in the deep sea will act to change ocean pH until the flux balance is restored. It is more difficult to preserve $CaCO_3$ in an acidic ocean. The timescale for ocean pH adjustment is 5–10 kyr, similar to the timescale of the recorded pCO_2 changes and definitely within the 100-kyr glacial/interglacial timescale. If (1) the glacial rate of weathering were higher, (2) $CaCO_3$ deposition currently occurring in shallow waters were shifted to the deep sea [*Berger*, 1982; *Berger and Keir*, 1984; *Opdyke and Walker*, 1992; *Kleypas*, 1997], or (3) the rate of $CaCO_3$ production decreased [*Keir*, 1988; *Archer and Maier-Reimer*, 1994; *Sigman et al*., 1998], $CaCO_3$ burial efficiency would increase and the ocean would become more basic. If organic carbon production increased, its degradation in sediments would also promote calcite dissolution [*Emerson and Bender*, 1981], further increasing ocean pH [*Archer and Maier-Reimer*, 1994]. $CaCO_3$ compensation may also affect the pCO_2 response to the biological pump scenarios described above [*Broecker and Peng*, 1987; *Boyle*, 1988b; *Keir*, 1988; *Sigman et al*., 1998].

We use an improved model of the ocean and sediment geochemical system to evaluate the effect of $CaCO_3$ compensation on these various ideas for lowering the pCO_2 of the glacial atmosphere. The ocean carbon cycle is a complicated system, controlled by biological processes we are only beginning to understand. Thus the formulation of the model is not completely constrained by our understanding of the underlying processes. Furthermore, we use the model to predict the sensitivity of the carbon cycle to climate and geochemical conditions which we are unable to observe except indirectly via clues preserved in the sedimentary record. The model, however, is the best that we are currently able to produce and does constrain the possibilities for the glacial carbon cycle. The model incorporates a new sedimentary diagenesis component which simulates the role of $CaCO_3$ compensation in determining atmospheric pCO_2, and a new iron cycle component, which predicts the effect of atmospheric iron deposition on carbon uptake by photosynthesis.

2. A MODEL OF THE OCEAN CARBON CYCLE: A GEOCHEMICAL PRIMER

This section constitutes a review of ocean geochemistry and the means by which it is incorporated into a numerical model. Table 1 summarizes the pertinent geochemistry, and Table 2 summarizes the hypotheses we will be testing. Some readers familiar with ocean chemistry may wish to turn directly to section 3.

2.1. Ocean Circulation

The flow of waters in the ocean, and the resulting exchange between the deep sea and the surface ocean, play a central role in determining the partitioning of carbon between the atmosphere and the ocean [*Heinze et al*., 1991] and the exchange time between the two (including the timescale for uptake of fossil fuel CO_2 in the coming centuries). The driving forces for ocean flow are (1) friction with winds and (2) density contrasts generated by differential heat and freshwater fluxes between

TABLE 1. Components of the Carbon Cycle Model

Component	*Description*
Ocean circulation	by adjoint circulation model fit to paleonutrient tracers ^{13}C and Cd
CO_2 pump	by photosynthesis in surface waters, limited by PO_4^{3-}, NO_3^-, or Fe; particles redissolve as they sink in the water column, and some small fraction lands on the seafloor; this process decreases pCO_2 of the atmosphere
$CO_3^=$ pump	by biological $CaCO_3$ formation in surface waters; more important in tropical waters and when H_4SiO_4 is unavailable (restricting competition by SiO_2-secreting diatoms); direct effect is to increase the pCO_2 of the atmosphere
$CaCO_3$ compensation	the ocean's way of balancing $CaCO_3$ burial against weathering (dissolved $CaCO_3$ input); increasing deep-sea $CO_3^=$ would increase $CaCO_3$ burial efficiency and lower pCO_2

the tropics and the poles. Much of the flow energy in the ocean is contained in 10- to 100-km-scale eddies [*Semtner and Chervin*, 1992], analogous dynamically to storms in the atmosphere. Unfortunately, the computational cost of resolving eddies is too high to include them in modeling studies which encompass the thousand-year overturning timescale of the ocean. Even without resolving eddies, the nonlinear terms in the fundamental equations of geophysical fluid motion are quite expensive to integrate over this time span. We show results from the large-scale geostrophic (LSG) global circulation model [*Maier-Reimer et al*., 1993], which parameterizes the effects of the eddy circulation field as diffusion and ignores many of the nonlinear inertial components of the equations of fluid flow, allowing a time step of a month on a computational grid that is 3.5° horizontally and on which there are 11 grid cells in the vertical, ranging from 50 m thick at the surface to 1000 m in the abyss. The LSG model clearly misses whole classes of sub-grid-scale motions, but it is particularly useful for reproducing the deep, long timescale circulation of the ocean. The LSG model resolves the seasonal cycle, but at the end of a model spin-up, the annual mean velocity field is recorded and used to advect tracers in an off-line tracer advection and geochemistry model called HAMOCC2 (Hamburg ocean carbon cycle) [*Maier-Reimer and Bacastow*, 1990]. The time step is a year, allowing easy access to the thousand-year timescales of interest for the global geochemistry of the ocean.

Ocean circulation during glacial time differed from today because the heat and freshwater fluxes, which determine the sea surface density field, were different. Deep-sea circulation is reconstructed using sedimentary "proxy" tracers which record past water conditions. Surface- and deep-living foraminifera leave geochemical proxies (as, for example, isotopic composition of carbon or boron or the concentrations of trace elements such as cadmium and barium) of the nutrient and CO_2 concentrations of the waters in which they grew [*Boyle*, 1988a; *Duplessy et al*., 1988; *Lea and Boyle*, 1990; *Sanyal et al*., 1995]. The chemistry of the deep Atlantic and Pacific, today distinguished from each other by the formation of freshly ventilated deep water in the North Atlantic, was more homogeneous during glacial time [*Curry and Lohmann*, 1982; *Duplessy et al*., 1988; *Boyle*, 1992; *Lea*, 1993]. As a result, the distribution of $CaCO_3$ on the seafloor was more uniform in the glacial ocean than it is today [*Berger*, 1973; *Broecker and Peng*, 1982; *Broecker*, 1993a]. Regional changes in the North Atlantic are well documented by an abundance of well-preserved $CaCO_3$ in the sediment and show that the depth of the transition between North Atlantic Deep Water and Antarctic Bottom Water was shallower, reflecting a shift in the relative densities of the northern and southern source waters or a decrease in the rate of deep convection in the North Atlantic. Circulation changes in the North Pacific [*Lynch-Stieglitz and Fairbanks*, 1994; *Keigwin*, 1998] and

TABLE 2. Glacial pCO_2 Scenarios

Scenario	*Description*
CO_2 pump scenarios	Fe fertilization of existing NO_3^- or PO_4^- pools in the ocean: This attains glacial pCO_2 values in box models, but not in circulation models, of the ocean carbon cycle.
	Increasing the NO_3^- pool of the ocean by 50%: This attains glacial pCO_2, but only for a few thousand years, until $CaCO_3$ compensation lowers the pH of the ocean. This scenario requires a major change in the biochemistry of phytoplankton during glacial time: the N:P (Redfield) ratio.
$CO_3^=$ pump scenarios	These ideas are supported by paleo-pH tracers (boron isotopes), but we have difficulty explaining how the implied glacial ocean pH increase was attained.
	Coral reef hypothesis: Lower sea level decreases in shallow-water $CaCO_3$ deposition, driving an increased $CaCO_3$ deposition in the deep sea. The increased ocean pH required to do this would lower pCO_2. However, deep-sea $CaCO_3$ burial rates from sediment cores do not appear to be high enough during glacial time.
	Rain ratio hypothesis: A decrease in $CaCO_3$ production, or an increase in organic carbon production, could shift ocean pH. A doubling of ocean H_4SiO_4 inventory could explain this, but we are unable to rationalize doubling H_4SiO_4. The predicted distribution of $CaCO_3$ on the seafloor is a poor fit to observations.

the Southern Ocean [*Francois et al*., 1998] are more difficult to document because of the paucity of $CaCO_3$ in the sediments in these locations.

2.2. Aqueous CO_2 Chemistry and the pCO_2 of the Atmosphere

CO_2 dissolved in water undergoes hydrolysis (the addition of H_2O) to form carbonic acid, H_2CO_3, which dissociates to bicarbonate (HCO_3^-) and carbonate ion ($CO_3^=$) [*Stumm and Morgan*, 1981]. Most of the dissolved carbon in seawater is in the form of bicarbonate. Carbonate ion is the form which controls the dissolution of $CaCO_3$, and dissolved CO_2 is the form which participates in gas exchange with the atmosphere. The pH equilibrium reactions of the carbonate buffer system can be simplified somewhat by defining two conservative quantities, the alkalinity and the total CO_2 concentration. Alkalinity is a charge balance condition, calculated from the proton-absorbing capacity of weak acids (mostly carbon and boron) relative to the specific end point where all the carbon is in undissociated form:

$$\text{alkalinity} = [HCO_3^-] + 2[CO_3^=] + [B(OH)_4^-].$$

Because the carbonate buffer equilibrium can be written as

$$CO_2 + H_2O + CO_3^= \leftrightarrow 2HCO_3^-,$$

additions of CO_2, such as by gas exchange, do not affect the alkalinity of the solution. The total CO_2,

$$\text{total } CO_2 = [CO_2] + [HCO_3^-] + [CO_3^=],$$

does respond to gas exchange but is conservative to changes in pH. The advantage of representing the chemistry of seawater using alkalinity and total CO_2 is that both are conservative to mixing, like simple tracers. These defined tracers are used both in the water column and in the sediment pore water components of the ocean model. The concentrations of CO_2 or $CO_3^=$ can be calculated from the alkalinity and total CO_2 values and are used to determine gas exchange and $CaCO_3$ equilibrium. The pCO_2 of a gas phase in equilibrium with a parcel of seawater increases with increasing total CO_2 concentration but decreases with increasing alkalinity.

Because the sea surface temperature and chemistry are heterogeneous, the steady state pCO_2 of the atmosphere is determined by balancing the regional fluxes across the air-sea interface. The situation is complicated further by differing exchange times of surface waters with waters of the deep sea, which is the largest ocean reservoir for CO_2. Simple box models of the ocean circulation (which impose circulation and exchange fluxes between a handful of well-mixed water masses in the ocean and allow for gas exchange with the atmosphere) have been used to develop a theory called the "high-latitude outcrop model" for the interaction of CO_2 between the ocean and the atmosphere [*Knox and McElroy*, 1984; *Sarmiento and Toggweiler*, 1984; *Siegenthaler and Wenk*, 1984]. The idea is that mixing between warm tropical surface waters and the deep sea is impeded by strong density stratification. In high latitudes the temperature contrast is less extreme between surface and deep, and water exchange is therefore easier. Because the high-latitude surface ocean is buffered by the great water mass of the ocean, the deep sea, the high latitudes are able to overwhelm the tropical surface ocean, which acts like a shallow, isolated pan of warm water, in determining pCO_2. In box models of the ocean the high-latitude surface ocean essentially controls the pCO_2 of the atmosphere; complete nutrient depletion in high-latitude surface waters generates pCO_2 of ~150 μatm, even lower than our glacial target of 200 μatm.

Three-dimensional ocean general circulation models (GCMs) for carbon cycle modeling do not exhibit the same high-latitude sensitivity as the box models [*Heinze and Broecker*, 1995; *Bacastow*, 1996; *Broecker et al*., 1999; *Archer et al*., 2000]. For this reason, the GCM used here predicts much higher pCO_2 when nutrients are depleted in high latitudes than the 150 μatm the box models would predict. The difference is vertical mixing, which provides a direct connection between the tropical surface ocean and the deep sea in GCMs which is absent from box models [*Archer et al*., 2000]. Vertical diffusion in the z-coordinate ocean circulation models is dominated by numerical mixing as fluid flows from one level to another of the computational grid. A new type of ocean circulation model has been formulated which discretizes the water column on density, or isopycnal, surfaces rather than on grid points of uniform depth [*Hu*, 1991], avoiding most of the vertical cross-grid flow and associated numerical diffusion. Isopycnic ocean carbon cycle models are expected to be more sensitive to the biological pump than z-coordinate models [*Archer et al*., 2000], if the vertical diffusion rate is specified to be low.

The question is, Which type of model best describes the real ocean? Field estimates of vertical mixing in the real ocean are contradictory. Turbulence microstructure measurements [*Gargett and Holloway*, 1984] and deliberate SF_6 tracer injection experiments [*Ledwell et al*., 1993] find low rates of diffusion, similar to the thermocline diffusivity used in the isopycnic model [*Hu*, 1996]. However, the density stratification of the thermocline and deep sea [*Munk and Wunsch*, 1998] and various geochemical measurements near the sea surface (such as oxygen [*Spitzer and Jenkins*, 1989] and helium concentrations [*Jenkins*, 1988]; measured rates of biological productivity [*Jenkins and Wallace*, 1992; *Emerson et al*., 1997]; and ocean distribution of natural and bomb radiocarbon [*Joos et al*., 1997]) imply a higher mean vertical diffusivity, similar to the rate of numerical mixing of the z-coordinate models. The discrepancy might be due to intense mixing near ocean boundaries and topography [*Munk and Wunsch*, 1998] or to transport within mesoscale eddies near the sea surface [*McGillicuddy and Robinson*, 1997; *Mahadevan and Archer*, 1998, 2000]. A low rate of vertical diffusion is found to be optimal for

simulating the density structure of the thermocline and the heat transport of the ocean [*Hu*, 1996], but *z*-coordinate GCMs with higher diffusivity do a fine job of simulating geochemical tracers which ought to be sensitive to diffusion (e.g., ^{14}C concentration of tropical surface waters and the global rate of biological export production). Until the long-term large-scale diffusivity of the real ocean is constrained to within a factor of 2 or so, we must regard the high-latitude pCO_2 sensitivity of the real ocean as an open question. If the real ocean is less diffusive than the numerical diffusion in the *z*-coordinate models, then achieving glacial pCO_2 values would be easier than what we present.

2.3. Organic Carbon Production and Export to the Deep Sea

Biological activity and its effect on the chemistry of seawater also play a fundamental role in determining the ocean/atmosphere partitioning of carbon. Photosynthetic phytoplankton in surface waters incorporate dissolved CO_2 into their tissue. These particles sink into the deep ocean to decompose back to CO_2. This process, called the biological pump [*Volk and Hoffert*, 1985], maintains a contrast in water chemistry between surface and subsurface waters. Because the atmosphere only sees the surface of the ocean, the biological pump decreases the pCO_2 of the atmosphere relative to what we would expect from an abiotic ocean (a thought experiment known in the business as the "Strangelove" ocean). The extent to which photosynthesis can draw down the CO_2 concentration of surface waters is limited by the availability of nutrients (what gardeners call fertilizers) including NO_3^-, PO_4^{3-}, H_4SiO_4, and various trace metals. As sinking biogenic particles degrade in the water column and in the sediments, they release their nutrients, maintaining a chemical gradient between surface and subsurface waters, just as for carbon.

The rate of carbon export as sinking particles from surface waters can be no greater than the rate of nutrient transport by upwelling of nutrient-rich deep water to the sea surface [*Dugdale and Goering*, 1967]. The ratio of NO_3^- to PO_4^{3-} in subsurface waters (about 16:1) is very similar to their proportions in living phytoplankton [*Redfield*, 1942]. In many parts of the surface ocean, residual PO_4^{3-} is present after NO_3^- is depleted [*Fanning*, 1992; *Gruber and Sarmiento*, 1997]. One proposal for lowering glacial pCO_2 is to raise the NO_3^- inventory of the glacial ocean until the biological pump reaches limitation by PO_4^{3-}, increasing the capacity of the biological pump [*Falkowski*, 1997]. A more radical proposal is to raise the NO_3^- inventory and release plankton from PO_4^{3-} limitation, by assuming that the plankton N/P ratio follows the chemistry of the seawater in which they grow [*Broecker and Henderson*, 1998]. This would allow a much larger increase in the strength of the biological pump.

The availability of iron plays a major role in the geochemistry of the oceans [*Martin and Fitzwater*, 1988; *Coale et al*., 1996]. While many parts of the ocean have nutrient concentrations near zero (i.e., limiting), other parts of the surface ocean retain significant concentrations of PO_4^{3-} and NO_3^-. In particular, the North Pacific, the equatorial Pacific, and the Southern Ocean stand out as "high-nutrient low-chlorophyll" (HNLC) areas [*Levitus et al*., 1993]. Iron is relatively insoluble in seawater, and so its concentration in upwelling seawater may be depleted relative to PO_4^{3-} and NO_3^- by loss of iron. The ocean iron cycle is replenished by atmospheric deposition as dust, the rate of which varies widely over the world oceans. Iron fertilization experiments, first in bottles of living surface seawater [*Martin and Fitzwater*, 1988] and then in unconfined in situ patches of water near the Galapagos Islands [*Martin et al*., 1994; *Coale et al*., 1996], have shown fairly decisively that at least in the equatorial Pacific the efficiency of the biological pump is limited by the availability of iron. Pelagic phytoplankton are thought to require an atom of iron for every 50,000–400,000 atoms of carbon [*Brand*, 1991; *Sunda et al*., 1991; *Sunda and Huntsman*, 1995].

The model in this study carries a suite of geochemical tracers intended to allow us to predict biological activity and the CO_2 concentration of surface waters (O_2, total CO_2, alkalinity, nutrient, Fe, H_4SiO_4, $\delta^{13}C$, and $\Delta^{14}C$). The model-predicted rate of organic carbon export production from the surface layer is based on the following assumptions. Acknowledging the near-parallel behavior of NO_3^- and PO_4^{3-} as nutrient tracers, the model only maintains one of the two. We can simulate the proposed glacial shift to NO_3^- limitation, or a change in the Redfield ratio of NO_3^- to PO_4^{3-}, by changing the ocean inventory in dissolved nutrient. Atmospheric dust supplies iron to the sea surface based on the present-day or the glacial simulations from *Mahowald et al*. [1999]. Total organic carbon export production is limited by NO_3^- or Fe, whichever is in shortest supply (Appendix 1). Light limitation is parameterized by decreasing the efficiency of nutrient and iron uptake in high latitudes [*Maier-Reimer and Bacastow*, 1990].

2.4. $CaCO_3$ and Opal Production

The pH-controlling mechanism, $CaCO_3$ compensation, is driven by the production and burial of $CaCO_3$. $CaCO_3$ is produced biologically, mostly in surface waters in association with photosynthesis. Rates of biological production vary widely in the oceans, and the reasons for this are not well understood and impossible to model mechanistically. However, some order emerges: The yields of organic carbon and $CaCO_3$ caught in sediment traps (which are like "rain gauges" on ocean moorings for catching sinking particles) are fairly well correlated, with a tendency toward a higher organic C:$CaCO_3$ ratio in regions of high production, such coastal upwelling zones, and cold places like the Southern Ocean [*Archer*, 1996b]. Factors which influence the organic C:$CaCO_3$ production ratio in the model include temperature and H_4SiO_4 availability.

A majority of the $CaCO_3$ is produced by coccolithophorid phytoplankton. Coccoliths compete against diatoms (algae which produce shells of opal (amorphous SiO_2)) for NO_3^- and PO_4^{3-}. Si (in the form H_4SiO_4) is typically depleted before NO_3^- and PO_4^{3-} in surface waters, leading to the conventional wisdom that under conditions of abundant dissolved H_4SiO_4 and iron, diatoms are able to outcompete coccoliths for NO_3^- and PO_4^{3-} [*Goldman*, 1984]. Therefore the H_4SiO_4 concentration of surface waters also plays some part in the rate of $CaCO_3$ production, because if H_4SiO_4 is available diatoms will get the NO_3^- and PO_4^{3-}.

In the model, opaline SiO_2 production is limited by the availability of H_4SiO_4 or by the limiting soft-tissue nutrient, NO_3^- or Fe. Using ideas developed by *Heinze et al*. [1999], the model assumes that opal sinks out of the surface ocean associated with NO_3^-, which is therefore unavailable to support the production of $CaCO_3$. Although the ratio of Si to N in diatoms varies in the real ocean, we adopt the *Nelson et al*. [1995] value of 1:1 as a global mean. After the Si-associated NO_3^- uptake is determined, we make the simplifying assumption that the nondiatom organic matter will be associated with $CaCO_3$ in a fixed ratio, which is determined by fit to the global distribution of alkalinity in the ocean. Overall, the relative production rates of organic C and $CaCO_3$ seem to be about 5:1 [*Li et al*., 1969]. Details are given in Appendix 1.

Most of the organic particles produced in surface waters decompose in the water column not too far from the sea surface. This can be measured using sediment traps [*Martin et al*., 1987] and checked using numerical models such as the one we present here. As sinking material decomposes, it releases its associated soft-tissue nutrients NO_3^- and PO_4^{3-}, and apparently iron [*Johnson et al*., 1997], while maintaining a greater proportion of SiO_2 and $CaCO_3$ in slowly dissolving shells. Sediment trap fluxes typically show little attenuation of the sinking flux of the $CaCO_3$ mineral calcite with depth [*Tsunogai and Noriki*, 1991], while the mineral aragonite appears to dissolve in the upper water column [*Betzer et al*., 1984]. The global production rate of $CaCO_3$ required by the ocean surface/deep alkalinity contrast is roughly a factor of 3 higher than the average allowable $CaCO_3$ rain rate to the seafloor required by the sediment diagenesis models (described below). We accommodate this need by allowing 30% of the $CaCO_3$ produced to sink to the seafloor with no attenuation and setting a 2000-m scale depth for the remainder.

Sinking SiO_2 also dissolves in the water column, more quickly in warmer waters than in colder waters. We use the analysis of *Gnanadesikan* [1999], who condensed a wide range of laboratory and field-based estimates of dissolution rates to the formula

$$R[\mathrm{day}^{-1}] = 1.32 \times 10^{16} e^{(-11481/T)}$$

and showed that this dissolution rate R coupled with a sinking rate of 50 m d^{-1} did a good job of reproducing the observed distribution of H_4SiO_4 in the world ocean.

The model also includes water-column release and scavenging of iron, based on the analysis of *Johnson et al*. [1997] and *Archer and Johnson* [2000]. Iron is released from sinking degrading organic matter along with NO_3^- and CO_2. In solution, iron appears to be removed by precipitation of colloidal particles or adsorption of iron onto existing particles (vaguely called "scavenging"), slowly at low Fe concentrations and faster as Fe exceeds a concentration of 0.6 nM. This behavior is apparently caused by complexation of the relatively insoluble Fe^{3+} by nanomolar concentrations of Fe-binding organic compounds detected and characterized by *Rue and Bruland* [1995]. The iron-binding strength of these compounds is similar to ligands produced by bacteria, algae, and fungi in terrestrial and freshwater systems, and an increase in the ligand concentration following iron addition in the open equatorial Pacific [*Rue and Bruland*, 1997] attests to the biological source of the open-ocean ligand species as well. The speciation of Fe^{3+} is calculated based on the depth-dependent distribution of two ligands detected by *Rue and Bruland* [1995], with observed binding constants $K_{L1} = [Fe - C_1]/[Fe][C_1] = 1.2 \times 10^{13}$ and $K_{L2} = 3.0 \times 10^{11}$. The rate of scavenging is assumed to be proportional to the concentration of unchelated Fe^{3+} with a rate constant (determined by model tuning) of 0.8 $year^{-1}$. Excess iron in surface waters (beyond the NO_3^- supported biological uptake) is removed to prevent lateral transport. The ocean model incorporating these iron dynamics predicts a high rate of iron recycling in the ocean (~70%), due entirely to the presence of these biogenic trace organic ligand species [*Archer and Johnson*, 2000].

2.5 Sediment Diagenesis

Once the biogenic particles reach the sediments, a whole new suite of physical and chemical processes controls their fate. We are interested in the burial of $CaCO_3$, which controls the pH of the ocean, and SiO_2, because H_4SiO_4 may play a role in determining $CaCO_3$ production. Most organic soft tissue reaching the seafloor degrades before it can be buried, and removal of carbon by organic matter burial is neglected by the model. However, organic carbon degradation plays a major role in $CaCO_3$ dissolution, necessitating its discussion here.

Solids in surface sediments are stirred by the actions of benthic deposit feeders, which ingest sediment wholesale to obtain a tiny fraction of the available organic matter there. Carbon 14 and ^{210}Pb in the solid phase document that the effect of solid mixing by bioturbation is analogous to diffusion acting over the top 5–20 cm of solid, with a diffusion constant D_B of 10–1000 cm^2 kyr^{-1}. These figures translate to a characteristic mixing time of hundreds of years [*Cochran and Krishnaswami*, 1980].

Within the surface sediments the chemistry of the

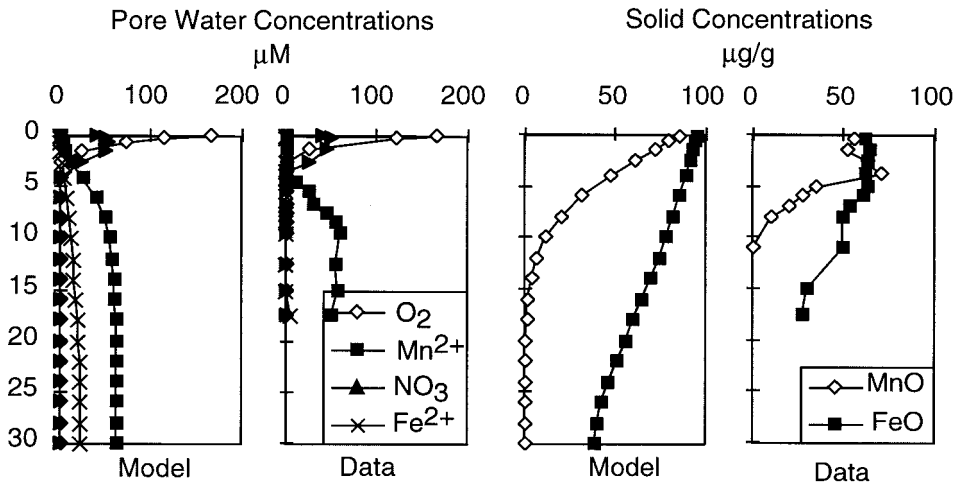

Figure 3. Model sedimentary pore water solute and solid phase concentration profiles compared with data from the central equatorial Pacific [*Froelich et al*., 1979].

pore water between the solid grains controls the rates of chemical reactions such as $CaCO_3$ and SiO_2 dissolution. The chemistry of the overlying water is a boundary condition for the differential equations which describe the depth-dependent chemical concentrations of pore water [*Berner*, 1980a]. This physics allows the rate of molecular diffusion to affect the rates of many sedimentary reactions, including the oxygen consumption by organic carbon respiration, and dissolution of $CaCO_3$ and SiO_2.

The interplay between organic carbon degradation and calcite dissolution is rather complicated, especially under high organic rain or low overlying water oxygen conditions. Oxic organic carbon degradation (respiration) produces CO_2, an acid, which reacts with pore water $CO_3^=$, promoting the dissolution of $CaCO_3$. In contrast, anaerobic organic carbon degradation has a smaller effect on the dissolution of $CaCO_3$ since electron acceptors such as NO_3^- (denitrification), MnO_2, Fe^{3+} solids, and SO_4^{3-} produce mostly HCO_3^- rather than CO_2. If the reduction products of these reactions, for example, dissolved reduced manganese (Mn^{2+}), diffuse upward and react with O_2, the net source of protons to the pore waters will be the same in most cases as if the initial respiration were oxic, but the depth distribution of the proton source will be different [*Canfield*, 1989].

The interesting behavior of the sediment model, with respect to atmospheric pCO_2, is found in the high organic carbon domain where suboxic diagenesis becomes important. We have addressed this need by incorporating into the ocean model a sediment diagenesis model for organic carbon, calcite, and opal which includes respiration by oxygen, nitrate, iron, manganese, and sulfate [*Froelich et al*., 1979]. The model diffusion/reaction equations and reaction kinetics are similar to previously published organic diagenesis models [e.g., *Burdige and Geiskes*, 1983; *van Cappellen and Wang*, 1996]. Model equations and reaction rate kinetics are given in Appendix 2, and concentration profiles of the model are compared with data in Figure 3.

2.6. $CaCO_3$ Compensation

We are now in a position to consider the details of the $CaCO_3$ mechanism for buffering the pH of the ocean. After an equilibration time of order 10,000 years, $CaCO_3$ compensation will have a profound impact on the effectiveness of any of the proposed mechanisms for generating glacial pCO_2 that we will consider. The idea is based on the mass balance of dissolved $CaCO_3$ flowing into the oceans from weathering and the removal of $CaCO_3$ from the ocean by burial. $CaCO_3$ is a base, and $CaCO_3$ dissolution on the seafloor will increase in an acidic ocean, at the expense of burial. An imbalance between sources and sinks of $CaCO_3$ to the ocean will drive the pH of the ocean toward restoring balance; for example, excess input of dissolved $CaCO_3$ will tend to drive the pH of the ocean toward the basic, increasing $CaCO_3$ accumulation on the seafloor until the rates return to balance. A basic ocean decreases pCO_2.

The solubility of $CaCO_3$ increases with increasing pressure, which tends to make the deepest waters of the ocean corrosive to $CaCO_3$. Because of this, $CaCO_3$ is preserved on topographic highs such as the mid-ocean ridges and tends to redissolve deep in the abyss [*Broecker and Takahashi*, 1978]. A map of $CaCO_3$ sediments resembles snowcapped mountains. Deep waters of the ocean accumulate CO_2 from decaying organic matter, making them more corrosive to $CaCO_3$. Recently formed deep waters in the Atlantic are less acidic than older Pacific deep waters, and the $CaCO_3$ "snow line" (called the carbonate compensation depth, or CCD) is deeper in the Atlantic than in the Pacific [*Archer*, 1996a]. The depth of the CCD is determined by the kinetics of dissolution from sediments. In the limit of infinitely fast dissolution kinetics the CCD would coincide exactly with

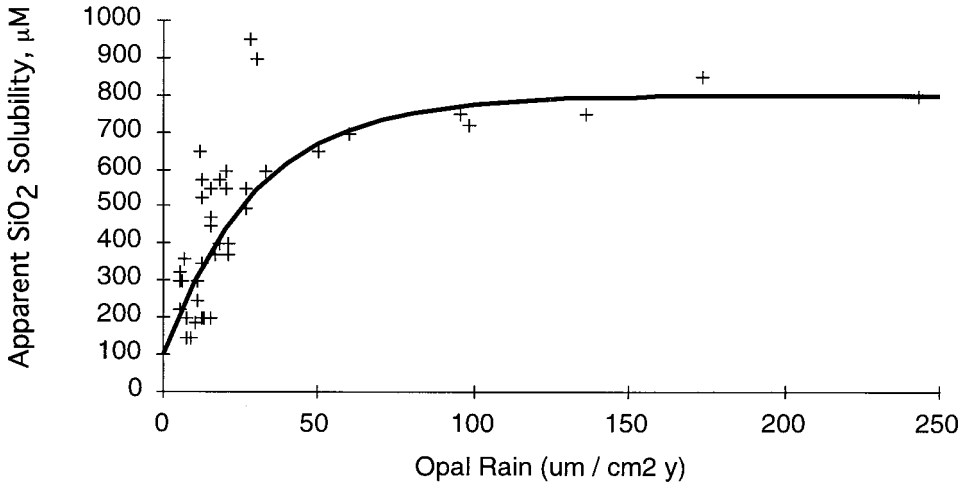

Figure 4. Apparent SiO_2 solubility, diagnosed from pore water profiles of dissolved Si in contact with measurable biogenic SiO_2 and at a depth of 10–20 cm in the sediment, effectively isolated from diffusive contact with the overlying water. SiO_2 produced in oligotrophic waters appears to be less soluble than SiO_2 from productive regions like the Southern Ocean. Data are from *Archer et al.* [1993] and *van Cappellen and Qiu* [1997]. Solid line is model parameterization.

the saturation horizon, but in the real world the CCD is found at some degree of undersaturation [*Archer*, 1996a].

$CaCO_3$ compensation can thus be quantified by combining the chemistry of the water column, which encompasses ocean circulation and biology, and of the dynamics of the sediments. The timescale for $CaCO_3$ compensation in the numerical model, calculated as the *e*-folding time for the model burial rate to relax to the imposed weathering input following fossil fuel invasion scenarios (acidifying the ocean), was found to be 5–10 kyr [*Archer et al.*, 1997].

2.7. Control of the Ocean H_4SiO_4 Inventory

The H_4SiO_4 concentration of the ocean, 150 μM in the deep Pacific, is considerably lower than the laboratory-measured solubility of biogenic opal (close to 1000 μM at 0°C [*Hurd et al.*, 1979]) and closer to the solubility for silicate clay minerals found in deep-sea sediments [*Sillen*, 1967]. For sedimentary clays to control the H_4SiO_4 concentration of the oceans, however, there would have to be a significant rate of Si uptake into clays. This process, called "reverse weathering," occurs too slowly for clays to be the primary controller of the ocean Si concentration. Therefore geochemists assume that the H_4SiO_4 concentration is maintained below saturation (with the relevant solid phase, biogenic opal) by biological Si uptake and burial in the oceans.

The mechanism that controls the concentration of Si in the world ocean is analogous to the $CaCO_3$ compensation mechanism for buffering ocean pH. Ocean chemistry is regulated by the requirement that burial in sediment balance influx due to terrestrial weathering. The concentration of H_4SiO_4 in the ocean functions as the homeostat, relaxing to the value at which SiO_2 burial balances supply by weathering. The residence time of Si in the model (the timescale for Si adjustment) can be calculated as the inventory (142×10^{15} mol) divided by the weathering rate (6×10^{12} mol yr^{-1}) to be 18 kyr.

Increasing the H_4SiO_4 concentration of the model ocean increases roughly linearly the rate of SiO_2 production and sinking to the seafloor. Once the SiO_2 lands on the seafloor, its preservation, always thermodynamically unfavorable, is a matter of competing kinetics of dissolution and removal from the undersaturated ocean by burial. The outcome of this competition can be predicted by the sediment diagenesis model. The simplest version of the model (Occam's favorite!) would take the solubility of the raining opal and its dissolution kinetics to be constant everywhere, varying only the rain rates and the overlying water chemistry to predict the distribution and burial of SiO_2. However, this model predicts that the opal concentration in sediments ought to scale with the opal rain rate squared, whereas it is observed that the opal concentration is nearly independent of opal rain rate until the rain rate reaches very high values, such as in the Southern Ocean [*Archer et al.*, 1993]. The culprit may be the solubility of opal, which can be determined from the pore water H_4SiO_4 concentration, in contact with measureable SiO_2, from deep enough in the sediment (10–20 cm) to be effectively isolated from diffusive contact with ocean water [*Archer et al.*, 1993]. This apparent SiO_2 solubility is found to vary systematically with the opal rain rate throughout the world oceans (Figure 4), as if the SiO_2 from productive regions were more soluble than SiO_2 from Si-starved areas. *Archer et al.* [1993] showed that the SiO_2 diagenesis model is able to reproduce the observed insensitivity of opal concentration and burial to opal rain rate over the observed range of tropical and subtropical SiO_2 rain rates, when the relationship between productivity and

solubility is included as a driver to the sediment model. Our ignorance of the mechanisms controlling SiO_2 solubility leaves us uncomfortable with including it here in a predictive model, but at least the model reproduces the observed dependence of SiO_2 burial to SiO_2 production. The simpler (Occam's) model would predict that the global ocean burial rate of SiO_2 would be more sensitive to the ocean Si content than does the model we show here.

3. MODEL APPLICATIONS

3.1. The Present-Day Ocean

The present-day ocean simulation provides a benchmark to evaluate glacial scenarios. The circulation field was generated using an adjoint to the LSG circulation model designed to minimize the difference between model phosphate concentration and core-top sedimentary Cd and $\delta^{13}C$ data [*Winguth et al*., 2000] (the same technique generated the LGM flow field, below). The model has been ground truthed to "ventilation" tracers (sensitive to contact with the atmosphere) such as ^{14}C and oxygen [*Maier-Reimer*, 1993]. Several model- or data-based maps of atmospheric iron deposition are available [*Duce and Tindale*, 1991; *Tegen et al*., 1996]. We use the present-day and glacial deposition field from *Mahowald et al*. [1999]. Only some fraction of the depositing iron is likely to be available to the biota, and we treat this fraction as a tunable parameter. A fraction of 6% produces the observed abundance of NO_3^- in surface waters, distributed as in Figure 5. The pCO_2 of the model atmosphere in the steady state is 276 μatm, close to the preanthropogenic value of 278 μatm. Another parameter is the weathering rate of dissolved $CaCO_3$ added to the ocean; this parameter is tuned to reproduce the present-day observed deposition rate of $CaCO_3$ in the deep sea (Figure 6a) and results in the distribution of $CaCO_3$ on the seafloor shown in Figure 6c. Summaries of the characteristics of all model runs are given in Tables 3 and 4.

3.2. The Glacial Ocean: The Model Starting Point

The glacial ocean differed from the present-day in several well-known ways, which we attempt to account for here, in construction of a glacial baseline model.

The glacial ocean was colder at the sea surface. High-latitude surface air temperatures (based on the Greenland ice core) were 10°–15° colder than at present, but the freezing point of water limits the expression of this colder climate on the upper ocean physics to an expansion of the cover of sea ice and near-freezing water. The tropics were also somewhat colder than today, although the magnitude of tropical cooling remains a point of some controversy. Estimates of tropical cooling seem to fall into a bimodal distribution, with one set of tracers (including species of planktonic microfossils preserved [*Climate: Long-Range Investigation, Mapping, and Prediction* (*CLIMAP*) *Project Members*, 1981], the oxygen isotopic ratio in $CaCO_3$ [*Broecker*, 1993a], and the chemistry of plankton membrane lipids preserved in sediments [*Bard et al*., 1997]) pointing to a cooling of only 1°–2°C and others (Sr/Ca in corals [*Guilderson et al*., 1994], noble gas concentrations in terrestrial aquafers [*Stute et al*., 1995], and tropical snow lines [*Rind and Peteet*, 1985]) saying the temperature changes were larger (4°–6°C). We will assume a tropical temperature 2°C colder than the CLIMAP reconstruction (Figure 7) and evaluate the sensitivity to that uncertainty (straight CLIMAP and CLIMAP −4°C in the tropics [see *Winguth et al*., 1999]). The direct effect of cooler tropics would be to lower the pCO_2 of the atmosphere by increasing the solubility of CO_2 gas.

Changing patterns of heat and freshwater fluxes also affected the circulation of the deep sea, which can be reconstructed using a suite of paleoceanographic "proxies" for past ocean chemistry. We use the best available glacial ocean flow field, called the "glacial second guess" velocities, based on glacial sedimentary ^{13}C and Cd/Ca data. The glacial flow field, like the interglacial field, was optimized by tuning the sea surface salinity field using an adjoint to the LSG circulation model [*Winguth et al*., 2000]. Overturning in the North Atlantic is shallower and about 30% slower than the interglacial flow field (Figure 8). One of the more prominent features of the glacial $\delta^{13}C$ distribution is extremely light values in the Southern Ocean (corresponding to high-nutrient, low-oxygen waters). These data are apparently inconsistent with glacial Cd data [*Boyle*, 1992; *Broecker*, 1993a], and the adjoint fit to the glacial ocean is unable to reconcile the two tracers.

There were differences in the bulk chemistry of the glacial ocean that we can also anticipate. Coral deposits from glacial time tell us that continental ice sheets sequestered enough water to lower the sea level by 120 m [*Fairbanks*, 1989]. Thus the concentrations of conservative salts and long-residence-time elements such as phosphorus increase by 3.14%; we assume that NO_3^- increased as well. This smaller size of the oceanic reservoir, and the decreasing solubility of CO_2 with increasing salinity, tend to increase atmospheric pCO_2, offsetting somewhat the pCO_2 drawdown associated with cooler sea surface temperatures.

The first step is to run the model until the water column and atmosphere reach steady conditions. Although the glacial iron deposition map increases the iron flux to the sea surface by a factor of 2.5 [*Mahowald et al*., 1999] (a bit lower than the *Rea* [1994] estimate based on deep-sea sediments), most of this increase goes to regions that already receive sufficient iron (i.e., are NO_3^- limited). The steady inventory of sea surface NO_3^- (surface to 50 m depth) decreases from 110×10^{12} mol in the present-day simulation to 80×10^{12} mol in the LGM baseline case, in a distribution shown in Figure 5c. A combination of colder sea surface temperatures and higher iron availability conspire to lower the pCO_2 of the

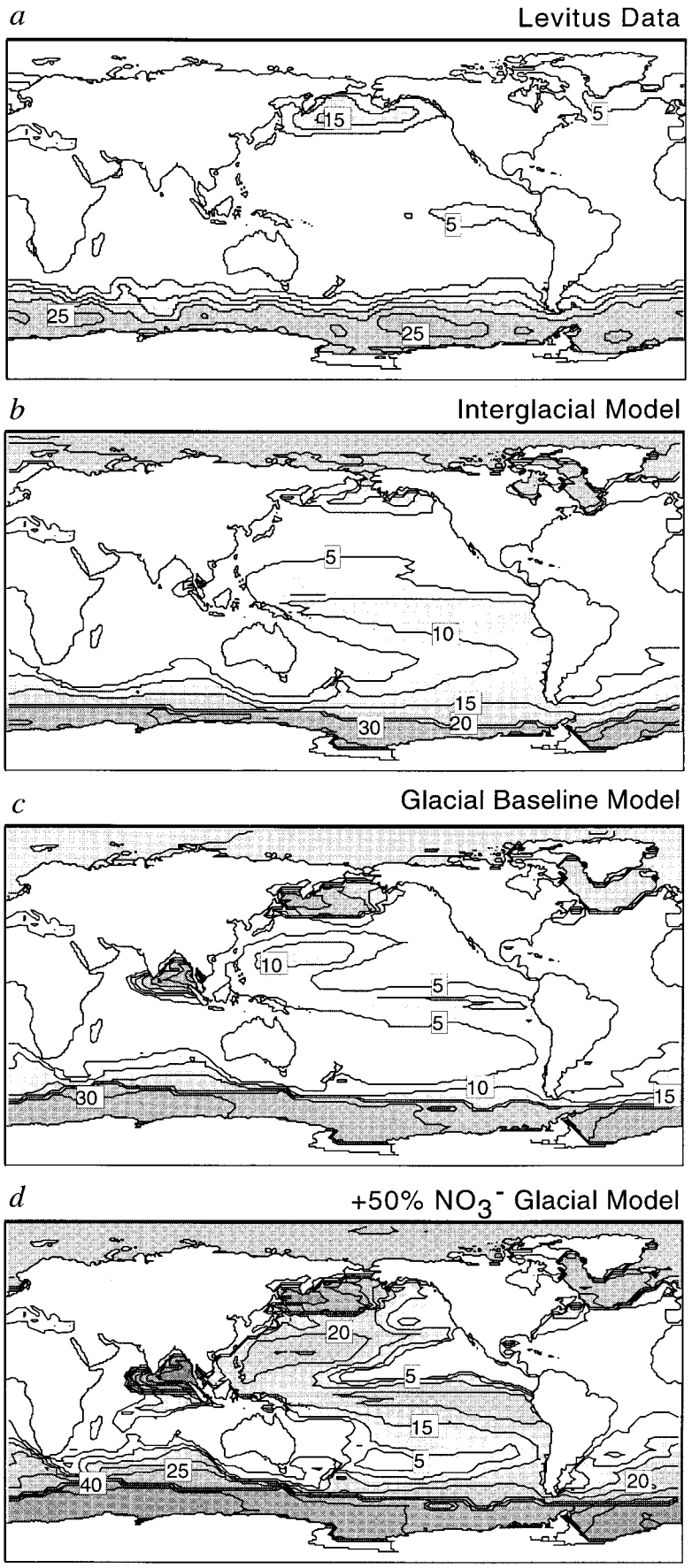

Figure 5. Sea surface NO_3^- concentrations. (a) Observed, derived from *Levitus et al.* [1993]. (b) Present-day model results. (c) Last Glacial Maximum (LGM) baseline model. (d) LGM NO_3^- + 50%.

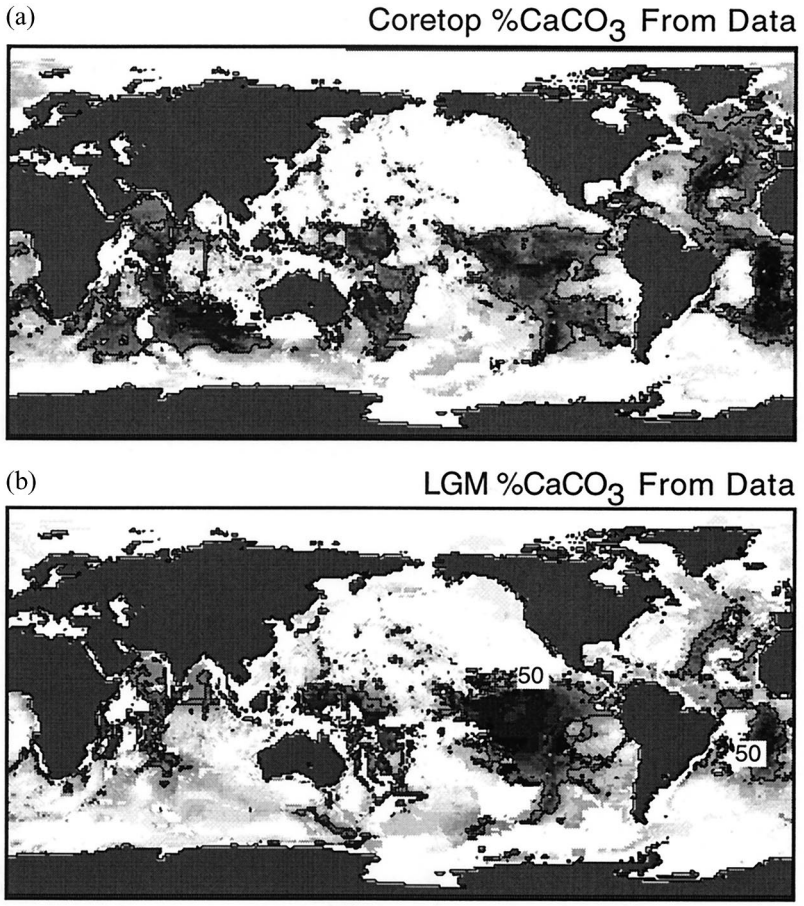

Figure 6. Distribution of $CaCO_3$ on the seafloor. (a) Present-day [*Archer*, 1996a]. (b) LGM reconstructed [*Catubig et al*., 1998]. (c) Present-day model. (d) LGM baseline model. (e) LGM weathering + 100%. (f) LGM H_4SiO_4 + 100%.

atmosphere to 268 μatm, a decrease of 8 μatm from the present-day simulation (Table 3 and Figure 9).

Next we account for changes in water chemistry that result from $CaCO_3$ and SiO_2 compensation, the ocean's way of balancing the $CaCO_3$ and SiO_2 removal rate against weathering. Although rates of weathering are not well known for the glacial world, our baseline assumption is that they were the same as today, and we will evaluate the sensitivity of pCO_2 to weathering fluxes below. We solve for the sediment-compensated steady state by adding or removing $CO_3^=$ and H_4SiO_4 until the burial rates of $CaCO_3$ and SiO_2 are restored to the rates predicted by the present-day model (22 and 8×10^{12} mol yr^{-1}, respectively) while evolving the steady states of the water column and atmosphere in response.

The LGM increase in iron deposition tends to increase all forms of biological production, including $CaCO_3$. Also, increasing the production of SiO_2 (by iron fertilization) and decreasing SiO_2 redissolution in the water column (by lowering tropical sea surface temperatures) increases SiO_2 burial by 70% (Table 4). The compensated ocean requires a 17% decrease in ocean H_4SiO_4 (Table 4), which has the effect of shifting production further toward $CaCO_3$. In the steady state the global ratio of $CaCO_3$ to organic C production in the model has increased from 0.198 in the present-day model to 0.210 in the steady glacial baseline model (Table 3). These changes tend to increase the production, deposition, and burial of $CaCO_3$. $CaCO_3$ compensation then demands that the pH of the ocean decrease until $CaCO_3$ burial is restored to the present-day value. The required acidification of the ocean overwhelms the direct water-column effect of iron fertilization, increasing pCO_2 to 280 μatm (4 μatm higher than the present-day simulation). We are far away from the glacial target of 200 μatm, and it gets worse.

3.2.1. Collapse of the terrestrial biosphere. It may be that the ocean had to accommodate changes in the carbon inventory of the terrestrial biosphere. The ratio of ^{13}C to ^{12}C in deep-sea $CaCO_3$ was approximately 0.4‰ lower during glacial time than at present [*Shackleton*, 1977; *Curry et al*., 1988]. The conventional interpretation is that during glacial time, some isotopically depleted biogenic organic carbon reservoir released approximately 40×10^{15} mol of carbon (500 Gt C), a 1% increase in the ocean/atmosphere carbon inventory. Possible sources include the terrestrial biomass (present inventory about 40×10^{15} mol C), soil organic carbon

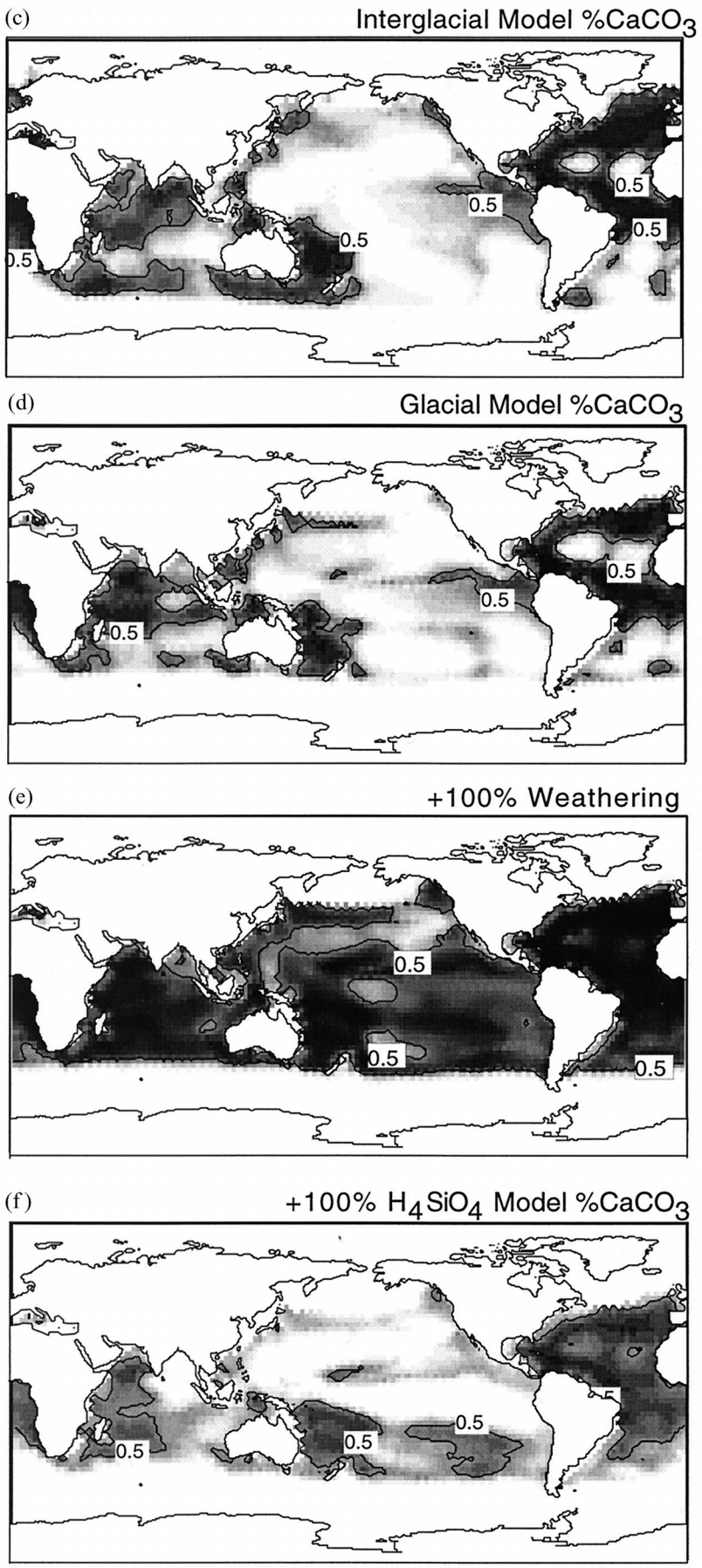

Figure 6. (continued)

TABLE 3. Summary of Model Results

	Production[a]			*pCO_2*[b]	
	Org	*$CaCO_3$*	*SiO_2*	*Uncompensated*[c]	*Compensated*[d]
Present-day	0.919	0.182	0.275	···	276
			Effect of Terrestrial C[e]		
LGM					
None	1.014	0.213	0.231	268	280
+500 Gt C[f]	1.014	0.213	0.234	305	297
+1000 Gt C	1.014	0.212	0.238	347	314
			Effect of SST[g,h]		
CLIMAP	1.000	0.206	0.241	307	295
Tropics − 2°[e,f]	1.014	0.213	0.234	305	297
Tropics − 4°	1.025	0.218	0.225	302	298
			Effect of Fe Deposition[e,h]		
Present Fe	0.990	0.207	0.234	310	305
Fe saturation	1.140	0.241	0.226	279	291
			Effect of NO_3^- Inventory[e,h]		
+50%	1.391	0.318	0.234	227	271
+100%	1.690	0.405	0.233	179	301
+200%	2.154	0.543	0.222	125	1025
			Effect of Weathering[e,h,i]		
+50%	1.014	0.204	0.265	···	265
+100%	1.014	0.198	0.289	···	242
+200%	1.014	0.189	0.325	···	193
			Effect of H_4SiO_4 Inventory[e,h,j]		
+100%	1.014	0.127	0.564	245	232
+150%	1.014	0.091	0.704	221	204
+200%	1.014	0.060	0.835	198	159
			Effect of H_4SiO_4 Inventory (No Terrestrial Carbon)[f,j]		
+100%	1.014	0.127	0.564	225	219
+150%	1.014	0.091	0.704	203	193
+200%	1.014	0.060	0.835	179	149

[a]Units of 10^{15} mol yr^{-1}.
[b]Units of μatm.
[c]Results from year 2000 of the simulation, after the atmosphere and the water column achieved steady state, but before sediment compensation.
[d]Sediment-compensated steady states, where $CO_3^=$ and H_4SiO_4 have been adjusted until $CaCO_3$ and SiO_2 burial rates match present-day values. For details, see Table 4.
[e]Using CLIMAP-2 flow field.
[f]Described in text as the glacial baseline model.
[g]CLIMAP sea surface temperatures adjusted in the tropics by 0°, −2°, or −4°C. The adjustment was uniform between 15°N and 15°S and decreased linearly with latitude to 0° at 25°N and 25°S.
[h]Assuming 40×10^{15} mol C from the terrestrial biosphere.
[i]Model runs have been sediment compensated to attain a multiple of present-day model $CaCO_3$ and SiO_2 burial rates.
[j]Only $CaCO_3$ burial is compensated to present-day values; SiO_2 burial is uncompensated.

(approximately 120×10^{15} mol), or sedimentary carbon on continental shelves, which were exposed during glacial time. Estimates of the change in the terrestrial biosphere based on models or reconstructions of the glacial world are generally higher than 40×10^{15} mol and range to 2 and 3 times the $\delta^{13}C$ value [*Crowley*, 1995].

The initial effect (before sediment compensation) of adding carbon to the atmosphere/ocean is to increase pCO_2 to 305 μatm (about 40 μatm per 40×10^{15} mol of C, the $\delta^{13}C$ based default) (Figure 9 and Table 3). Reaction with $CaCO_3$ tends to neutralize this added CO_2, just as it will neutralize fossil fuel CO_2 in the coming centuries, resulting in an ultimate increase to 297 μatm, an increase of 17 μatm. We will conduct our exploration of glacial pCO_2 sensitivity under the assumption that the terrestrial biosphere contributed 40×10^{15} mol C to the ocean/atmosphere system, consistent with the $\delta^{13}C$ results. The bottom line is that we are beginning our search for lower glacial pCO_2 from a "glacial baseline" pCO_2 of 297 μatm, which is 20 μatm higher than the present-day model value. Note that if the carbon came from marine organic matter stored in continental shelf sediments exposed by lowered sea level, and if this material contained a Redfield proportion of PO_4^{3-}, then the PO_4^{3-} concentration of the ocean should

have increased by approximately 10%. Assuming a corresponding increase in NO_3^-, this lowers pCO_2 from 297 μatm down to 295 μatm after compensation.

The increase in CO_2 solubility in a colder glacial ocean, and the increase in iron deposition from the arid glacial climate, have been of only marginal help, and the terrestrial carbon reservoir if anything takes us in the wrong direction from reaching the glacial pCO_2 of 200 μatm.

3.2.2. Tropical temperatures. In contrast to the terrestrial carbon contribution, the pCO_2 of the atmosphere is relatively insensitive to uncertainty in the temperature of the tropical sea surface; pCO_2 decreases by 5 μatm as tropical temperatures cooled over 4°C (Figure 9). However, tropical cooling alters biological production (organic carbon increases because of a decrease in stratification, and SiO_2 decreases because temperature-dependent SiO_2 dissolution kinetics decrease upper water column H_4SiO_4 recycling) in ways which prompt sediment compensation to increase pCO_2 as tropical temperatures drop (reversing the trend). Even ignoring this effect, the sensitivity of pCO_2 to tropical cooling is small compared with our goal of 200 μatm.

TABLE 4. Details of Sediment Compensation in the Model Runs

	Precompensation Burial[a]		*Compensated Inventories*[b]	
	$CaCO_3$	*SiO_2*	*Alk*	*H_4SiO_4*
Present-day	21.9	8.0	3546	142
Effect of Terrestrial C[c]				
LGM				
None	27.2	13.5	3484	119
+500 Gt C[d]	18.7	12.1	3562	120
+1000 Gt C	12.8	11.1	3638	122
Effect of SST[e]				
CLIMAP	17.4	11.8	3575	121
CLIMAP-2[d]	18.7	12.1	3562	120
CLIMAP-4	19.8	12.5	3550	119
Effect of Fe Deposition[c,e]				
Present-day Fe	19.8	12.3	3551	120
Fe saturation	24.4	13.8	3495	116
Effect of NO_3^- Inventory[c,e]				
+50%	41.5	14.8	3344	120
+100%	69.8	17.1	3024	120
+200%	129	20.0	2054	114
Effect of H_4SiO_4 Inventory[c,e,f]				
+100%	15.0	52.8	3756	285
+150%	15.0	83.3	3893	356
+200%	13.0	115.4	4300	427
Effect of H_4SiO_4 Inventory (No Terrestrial Carbon)[c,e]				
+100%	17.5	···	3680	
+150%	17.0	···	3818	
+200%	14.4	···	4232	

[a]Units of 10^{12} mol yr^{-1}. Burial rates are adjusted to match present-day model results by adjusting the alkalinity and H_4SiO_4 inventories of the ocean.
[b]Units of 10^{15} eq (alkalinity) or 10^{15} mol (H_4SiO_4).
[c]Using CLIMAP-2 flow field.
[d]Described in text as glacial baseline run.
[e]Assuming 40×10^{15} mol terrestrial C added to the ocean.
[f]Only $CaCO_3$ burial is compensated to present-day values; SiO_2 burial is uncompensated.

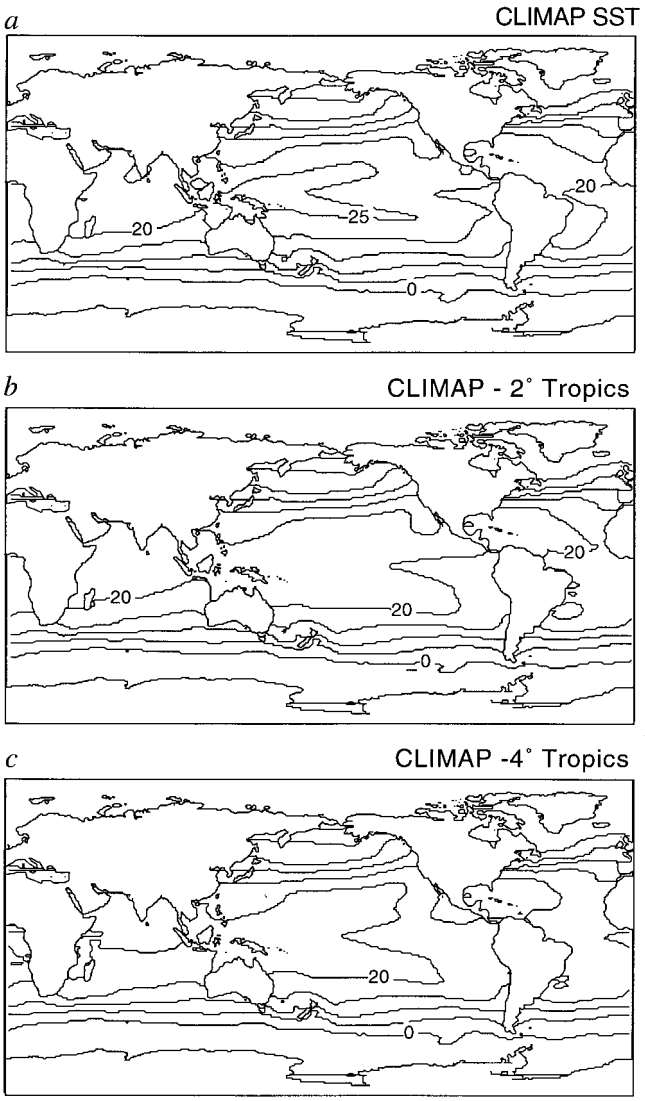

Figure 7. Sea surface temperatures. (a) Climate: Long-Range Investigation, Mapping, and Prediction (CLIMAP). (b) CLIMAP with 2°C of tropical cooling (2°C subtracted from CLIMAP sea surface temperature (SST) between 15°N and 15°S latitudes, with a linearly decreasing temperature adjustment between 15° and 25° north and south latitudes. (c) CLIMAP − 4°C, constructed as in Figure 7b. See *Winguth et al.* [1999] for details.

3.3. Biological Pump Scenarios

The first family of glacial pCO_2 scenarios, which has been on the table in various forms since the beginning, proposes an increase of the CO_2 contrast between surface ocean waters and the deep sea maintained by biological activity in the ocean. This would result in more carbon storage in the huge CO_2 reservoir of the deep sea. There are two possible strategies, outlined in Table 2. One is to release the ocean from iron limitation,

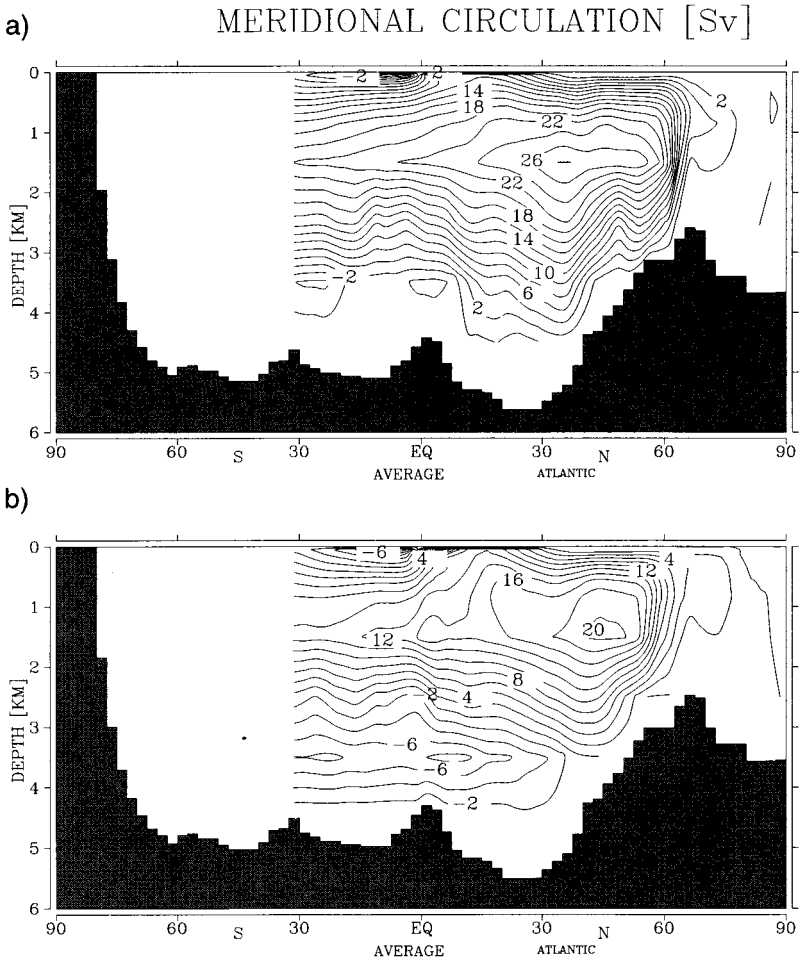

Figure 8. Optimized overturning circulation of the Atlantic Ocean, (a) interglacial, and (b) glacial, from *Winguth et al*. [2000]. Overturning in the North Atlantic was shallower and slower in this reconstruction.

enabling it to utilize the existing inventories of NO_3^- and PO_4^{3-} more effectively. The second is to increase the inventory of NO_3^- by increasing nitrogen fixation or decreasing denitrification.

3.3.1. Iron fertilization. Iron appears to be limiting uptake of NO_3^- and PO_4^{3-} in surface waters of the equatorial Pacific, the North Pacific, and the Southern Ocean. Ice cores [*Peteet et al*., 1990] and deep-sea sediments [*Rea*, 1994] tell us that the deposition of dust was higher during glacial time, probably because the glacial world was more arid than today [*Sarnthein*, 1978; *Mahowald et al*., 1999]. The iron hypothesis for glacial pCO_2 is especially attractive when coupled to the high-latitude outcrop theory, which says that pCO_2 is particularly sensitive to forcing from the Southern Ocean. The discovery that the rate of iron deposition in the snows of Antarctica was an order of magnitude higher during glacial time [*Peteet et al*., 1990] tied the iron hypothesis and the high-latitude outcrop model into a neat bundle that is still very compelling and is in fact probably the canonical favorite scenario among the paleoceanographic community today. This scenario might work if the ocean behaves as a box model, but we shall see that the pCO_2 response of the GCM is too weak for fertilization to explain glacial pCO_2.

3.3.1.1. Paleoceanographic evidence: Fe fertilization fits with the sequence but not the timing of events during the last two deglaciations [*Sowers et al*., 1991; *Sowers and Bender*, 1995], and in particular termination II (the penultimate deglaciation) [*Broecker and Henderson*, 1998]. The first indication of termination II was a decrease in dust accumulation in Antarctic snow (Figure 2). The pCO_2 remained steady at 200 μatm until the dust began to decrease, when pCO_2 began to rise toward interglacial levels. Several thousand years after pCO_2 began to rise, ^{18}O of O_2 in the atmosphere tells us that the ice sheets began to melt. The sequence of termination I is similar but somewhat less clear [*Sowers and Bender*, 1995]. By 14.5 kyr the pCO_2 transition was 60% complete, while sea level was only 20% toward interglacial levels.

The sequence is consistent with pCO_2 increase caused by iron limitation in the Southern Ocean, but the timescale of the pCO_2 increase does not fit very well. The transition to interglacial pCO_2 took 7–14 kyr at termination II and 6–7 kyr at termination I [*Sowers and Bender*, 1995]. The timescale for CO_2 equilibration be-

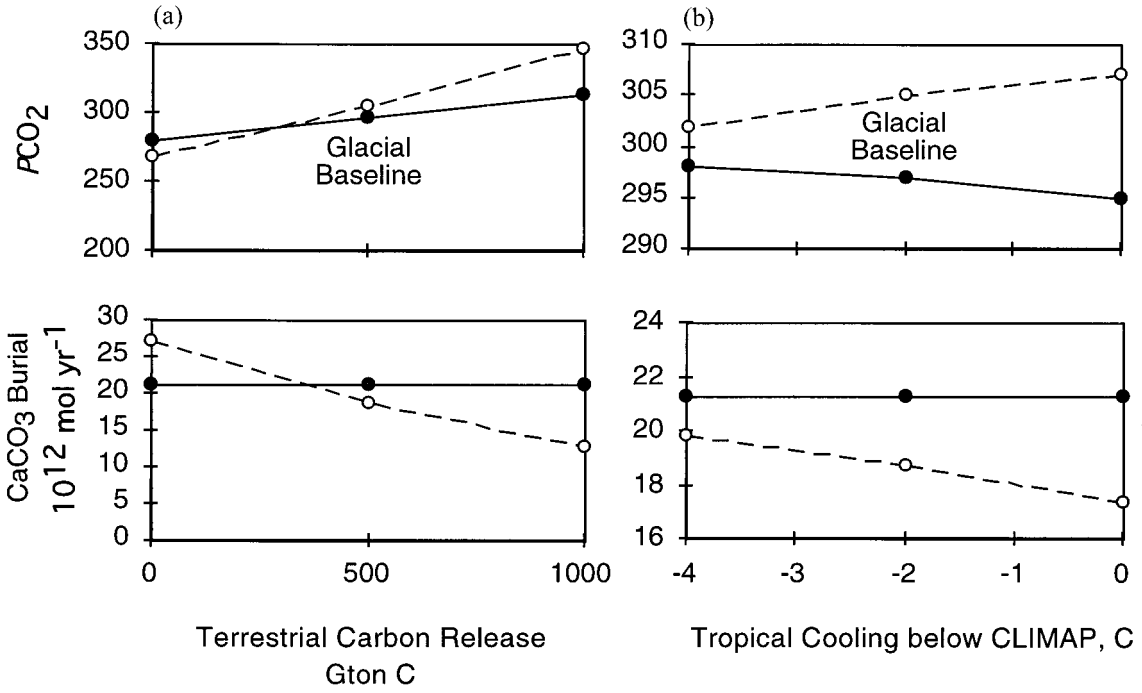

Figure 9. The pCO_2 and $CaCO_3$ burial sensitivity to tropical sea surface temperature and carbon release from the terrestrial biosphere. Open circles represent uncompensated (water column only) steady state, where $CaCO_3$ burial is allowed to deviate from the (assumed constant) weathering flux. Solid circles are the model state after ocean pH has adjusted to restore $CaCO_3$ burial to the weathering rate. See also Tables 3 and 4. (a) Effect of terrestrial C, using the CLIMAP-2 flow field. (b) Effect of SST, assuming 40×10^{15} mol C from a decrease in the terrestrial biosphere.

tween the atmosphere and the ocean (neglecting second-order effects like buffering by $CaCO_3$) is hundreds of years [*Maier-Reimer and Hasselmann*, 1987]. A biological pump scenario for increasing pCO_2 over a 10-kyr timescale would therefore have to be paced externally, say, by a 10-kyr timescale change in iron delivery, which is not obvious in the dust records.

3.3.1.2. Model results: The glacial baseline model, using the *Mahowald et al*. [1999] iron deposition field, does not generate glacial pCO_2. We can isolate the model sensitivity to iron by running the same model configuration (glacial flow and sea surface temperatures) using the present-day iron deposition field as a low extreme, and with complete iron saturation (NO_3^- limitation) as an upper bound (Table 3). In the initial water-column spin-up, present-day iron fluxes increased pCO_2 by 5 μatm to 310 μatm, while saturation of iron decreased pCO_2 by 26 μatm to 279 μatm (this result and all following assume 40×10^{15} mol C released from the terrestrial biosphere, consistent with $\delta^{13}C$).

Sediment compensation tends to minimize the pCO_2 response to Fe deposition. An increase in production, for example, increases the global burial rate of $CaCO_3$ above the assumed constant weathering rate as it lowers pCO_2 (Table 4). Balance between influx and burial of $CaCO_3$ is achieved by acidifying the ocean, increasing pCO_2. Sediment compensation thus restores pCO_2 to 291 μatm, restoring 12 of the 26 μatm pCO_2 removed in response to the glacial increase in iron deposition. Iron fertilization by itself appears insufficient to drive pCO_2 to the glacial level of 200 μatm, which is especially true if we accept the terrestrial carbon contribution of 40×10^{12} mol of C. The potential of the biological pump to decrease pCO_2 during glacial time, a mainstay of paleoceanographic theory [*Broecker*, 1982b], is weakened by the effects of $CaCO_3$ compensation [*Keir*, 1988; *Sigman et al*., 1998].

3.3.2. Can we monkey with the glacial NO_3^- inventory? An astonishing feature of ocean chemistry is that the ratio of NO_3^- to PO_4^{3-} in deep waters is remarkably close to its ratio in living phytoplankton (this stoichiometry is known as the Redfield ratio [*Redfield*, 1942]). PO_4^{3-} has the longer residence time in the ocean (approximately 100,000 years), determined by the rates of input by terrestrial weathering and removal by various mechanisms in sediments [*Froelich et al*., 1982]. NO_3^- has biological sources and sinks by conversion to and from the relatively inert form N_2. Nitrogen fixation is the production of NH_4 from N_2 and occurs primarily in stratified nutrient-depleted tropical and subtropical surface waters [*Capone et al*., 1997]. Denitrification, the loss of NO_3^- to N_2, is the microbial use of NO_3^- as an electron acceptor in anaerobic respiration. This occurs primarily in low-oxygen waters and in shallow-water coastal and continental margin sediments. The residence time of

NO_3^- is an order of magnitude shorter than it is for PO_4^{3-} (3–10 kyr).

The shorter residence time of NO_3^- supports a "geochemist's" viewpoint that ultimately the inventory of PO_4^{3-} must be limiting to biological production, because NO_3^- can be generated relatively quickly (on geological timescales) by biological processes that might be responsive to PO_4^{3-} limitation, tending to maintain the ratio of NO_3^- and PO_4^{3-} in seawater close to the Redfield ratio. Many geochemists assume that if the PO_4^{3-} concentration of the ocean were higher, nitrogen fixers would take advantage of the opportunity to fix more nitrogen, driving the ocean NO_3^- concentration up toward Redfield balance with the inventory of ocean PO_4^{3-}. On the shorter term and on a smaller scale, however, the picture looks different; many parts of the surface ocean retain small concentrations of PO_4^{3-} even after NO_3^- has been exhausted [*Fanning*, 1992; *Gruber and Sarmiento*, 1997], leading to a "biologist's" conclusion that NO_3^- is limiting.

The sources and sinks of NO_3^- may be sensitive to glacial timescale changes in climate and ocean chemistry [*McElroy*, 1983; *Broecker and Henderson*, 1998]. Nitrogen fixation requires iron as an enzyme cofactor, and metabolic iron requirements of nitrogen fixers are high [*Falkowski*, 1997]. Locations of nitrogen fixation in the ocean today can be diagnosed from historical measurements of NO_3^- and PO_4^{3-}, as deviations in the NO_3^- to PO_4^{3-} ratio from the ocean mean [*Gruber and Sarmiento*, 1997]. These patterns reveal that nitrogen fixation occurs in tropical sea surface areas of abundant iron flux from continental dust, for example, in the subtropical Atlantic off the Sahara desert. The increased dustiness of the glacial world might favor nitrogen fixation, but a decrease in the area of warm tropical surface waters could decrease nitrogen fixation.

The global rate of denitrification depends on the oxygen concentration of the deep sea and the geometry of the seafloor relative to zones of low oxygen. An increase in the biological pump would tend to decrease oxygen concentrations, increasing denitrification. However, this tendency could be offset by a source of ventilated (high oxygen) waters to intermediate layers of the ocean where denitrification occurs today [*Kennett and Ingram*, 1995]. The best clue we have to the state of denitrification during glacial time comes from the isotopic composition of nitrogen. Denitrification is accompanied by a strong isotope effect (−30‰) which tends to enrich any unutilized NO_3^- in the heavier isotope ^{15}N. In sediments where denitrification occurs, all or most of the nitrate in the pore waters is consumed, leaving behind no residual nitrate to carry the isotopic signature of the fractionation [*Brandes and Devol*, 1997]. Water-column denitrification, in contrast, often proceeds only partially to completion, leaving behind an isotopic signature of denitrification that can be detected above the oxygen minimum zone waters in the eastern equatorial Pacific [*Ganeshram et al*., 1995] and the Arabian Sea [*Altabet et al*., 1995]. These signatures are missing from glacial sediments in these cores, implying a decrease in denitrification, perhaps because oxygen concentrations were higher in intermediate waters (at least in the North Pacific [*Kennett and Ingram*, 1995]).

Globally, in steady state, the isotopic ratio of NO_3^- in the deep sea is determined by the constraint that the isotopic ratio of the sources (near 0‰) balance that of the sinks (which equals ocean $\delta^{15}NO_3^- - 30‰$ for water-column denitrification and $\delta^{15}NO_3^- - 0‰$ for sedimentary denitrification). If all of the denitrification occurred in sediments where NO_3^- is completely utilized, then the deep-sea $\delta^{15}NO_3^-$ would be near 0‰; if it occurred primarily in water-column settings where reaction proceeds only partly to completion, then ocean NO_3^- could reach +30‰. The isotopic ratio of deep-sea NO_3^- during glacial time can be inferred from the $\delta^{15}NO_3^-$ in sediments under oligotrophic regions, where NO_3^- is completely consumed, and where therefore the fractionation associated with biological uptake (a different effect from denitrification fractionation) is not expressed. Oligotrophic sedimentary $\delta^{15}NO_3^-$ from glacial time is +5–6‰ (M. Altabet, personal communication, 1998), similar to the $\delta^{15}NO_3^-$ of the deep sea today [*Altabet and Curry*, 1989], suggesting that the balance of sedimentary to water-column denitrification, globally, in the glacial ocean, was similar to today's ocean.

One proposal for generating low glacial pCO_2 is to increase the NO_3^- concentration of the ocean, until PO_4^{3-} becomes limiting [*Falkowski*, 1997]. The effect of releasing the ocean from NO_3^- limitation can be calculated from the potential sea surface PO_4^{3-} drawdown (from a present-day residual of, say, 0.1 μmol kg^{-1} down to zero) divided by the deep-ocean value (2.5 μmol kg^{-1}), an increase in the effective global pool of ocean nutrient of order 4%.

A second possibility is that the ratio of NO_3^- to PO_4^{3-} in phytoplankton might be determined by the water chemistry, rather than the more traditional interpretation that it is the chemistry of phytoplankton that determines the chemistry of the ocean. Phytoplankton grown in laboratory vats take up luxury phosphorus in excess of their apparent requirements: When NO_3^- to PO_4^{3-} is increased beyond the Redfield ratio, the plankton take the extra nitrogen, up to a point (when P becomes truly limiting) [*Rhee*, 1978; *Elser and Hassett*, 1994]. The idea is that an increase in iron supply to the surface ocean stimulates an increase in nitrogen fixation, generating an increase in the $NO_3^-:PO_4^{3-}$ ratio of the deep sea, and an increase in the effective nutrient reservoir of the ocean, by perhaps a factor of 2. The constancy of N:P ratios in seawater and in marine plankton [*Hecky et al*., 1993], however, fuels considerable skepticism that the Redfield ratio is really negotiable.

3.3.2.1. Model results: Beginning with the glacial baseline model, including a terrestrial carbon contribution of 40×10^{15} mol C, we subjected the model to increases in the ocean inventory of NO_3^- and ran until $CaCO_3$ and SiO_2 burial balanced the weathering fluxes

(Figure 10). Here $CaCO_3$ compensation works strongly against lower pCO_2 values, a tendency also observed by *Sigman et al*. [1998]. A 50% increase in nutrient inventory initially draws pCO_2 down to 227 μatm. The increase in NO_3^- drove organic C production to 1.39×10^{15} mol yr^{-1}, up by 37%, increasing $CaCO_3$ production and burial. Also, because the inventory of H_4SiO_4 is the same as in the glacial baseline model, the ratio of NO_3^- to H_4SiO_4 increases, increasing the ratio of $CaCO_3$ to organic carbon production (from 0.210 to 0.228), further increasing $CaCO_3$ burial. Most significantly, the decrease in deep-water oxygen concentration shifted much of the sedimentary respiration from oxic chemistry, which promotes $CaCO_3$ dissolution, to suboxic reactions, which have less effect on pore water pH. The sum of these three effects is to nearly double the rate of $CaCO_3$ burial in the uncompensated ocean (Table 4 and Figure 10). The compensation response is to lower the pH, increasing dissolution until burial balances the same rate as the original present-day model. This acidification also increases the pCO_2 of the atmosphere to 271 μatm. For the doubled and tripled NO_3^- scenarios the $CaCO_3$ effect is even more pronounced, to the point where increasing the ocean NO_3^- inventory actually increases the ultimate pCO_2 of the atmosphere rather than decreasing it (Table 3 and Figure 10).

3.3.2.2. Paleoceanographic evidence: If there were more NO_3^- in the ocean, then presumably iron limitation would become more important, and sea surface NO_3^- concentrations would increase (Figure 5). Paleo-sea-surface NO_3^- concentrations can be inferred from sedimentary nitrogen isotope data. Nitrate uptake by phytoplankton is associated with a 2.5‰ isotopic fractionation, leaving behind NO_3^- that is heavier, depending on the extent of NO_3^- depletion [*Altabet and Francois*, 1994]. Glacial $\delta^{15}N$ values from the Southern Ocean indicate a greater degree of nutrient utilization [*Francois et al*., 1998] (the opposite of the model results), while equatorial Pacific $\delta^{15}N$ shows lower nutrient utilization efficiency [*Farrell et al*., 1995].

Stable carbon isotopes can also be used as a tracer for biological activity in the ocean. The isotopic ratio of carbon in dissolved CO_2 differs between the surface and the deep ocean, and this fractionation is expected to increase with an increase in the biological pump. The $\delta^{13}C$ as recorded in $CaCO_3$ is affected by (1) the terrestrial carbon contribution [*Shackleton*, 1977], which offsets surface and deep $\delta^{13}C$ equally, (2) biological fractionation associated with photosynthesis [*Shackleton et al*., 1983], (3) gas exchange with the atmosphere [*Broecker and Maier-Reimer*, 1992; *Charles et al*., 1993; *Lynch-Steiglitz et al*., 1995], and (4) an artifact in the recording of dissolved $\delta^{13}CO_2$ by planktonic foraminifera which correlates with the $[CO_3^{=}]$ or pH of the water in which they grow [*Spero et al*., 1997; *Lea et al*., 1999]. Sea surface $\delta^{13}C$ becomes much more variable in the 50% increase NO_3^- model glacial ocean, in correlation with variability in NO_3^- concentration, but if we take an average of $\delta^{13}C$ from 30°N to 30°S, we see that, in accord with W. Broecker et al. (manuscript in preparation, 1999), a combination of a 40×10^{15} mol C terrestrial carbon contribution (point 1), an increase in the biological pump resulting from a 50% increase in ocean NO_3^- (point 2), and the pH artifact (point 4) conspire to maintain sea surface $\delta^{13}C$ near present-day values, more or less as observed (Table 5).

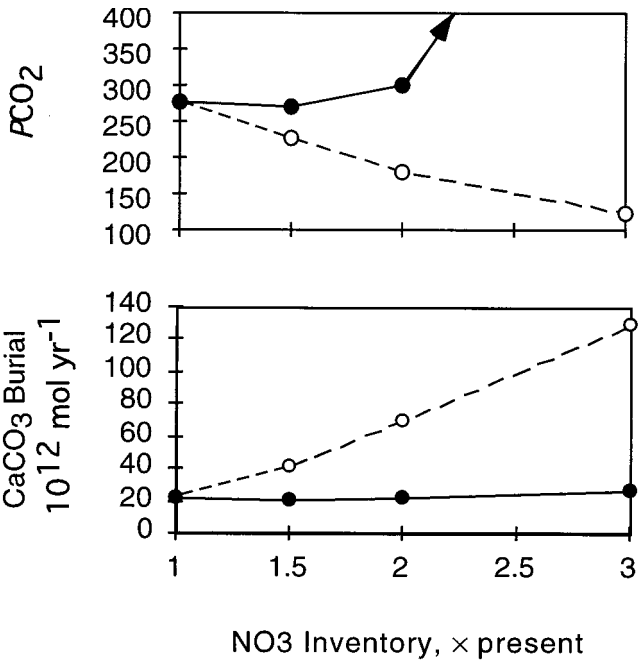

Figure 10. The pCO_2 and $CaCO_3$ sensitivity to the ocean NO_3^- inventory, assuming no PO_4^{3-} limitation. NO_3^- is not added to or lost from the model; its inventory is specified as an initial condition. These runs use the CLIMAP-2 flow field and assume the addition of 40×10^{15} mol C from the terrestrial biosphere. See also Tables 3 and 4. Open circles are uncompensated (water column steady state), and solid circles are sediment compensated (where $CaCO_3$ and SiO_2 burial rates balance present-day model results). When the NO_3^- inventory increases, pCO_2 is initially drawn down, but $CaCO_3$ burial exceeds weathering. Compensation restores burial to the weathering rate by acidifying the ocean, negating the initial pCO_2 drawdown.

Another potential indicator of the strength of the biological pump during glacial time is the oxygen concentration of deep water, specifically the extent of anoxic waters in the deep sea. The circulation model is not especially good at predicting anoxia, because there is a tendency to generate anoxia even in the present-day simulation, where there is none in the real ocean [*Najjar et al*., 1992; *Six and Maier-Reimer*, 1996]. For what it's worth, however, the glacial flow field reduces the extent of anoxia in the ocean because of an acceleration in the ventilation of the thermocline (Table 6). Increasing the inventory of NO_3^- by 50% increases the extent of anoxia to 60% greater than the present-day model results. Far from definitive, these results warn us that oxygen concentrations are a function of circulation as well as of

TABLE 5. Carbon Isotopic Response to Higher Nutrient Scenario, Sea Surface Values Relative to Present-Day Model Results

	$\Delta\delta^{13}C_{atm}$	$\Delta\delta^{13}C_{avg}$[a]	$\Delta\delta^{13}C_{avg}$ (*sacculifer*)[b]
LGM baseline[c]	−0.7	−0.56	−0.39
NO_3^- + 50%	+0.2	−0.03	+0.18
H_4SiO_4 + 100%	−0.5	−0.57	−0.65
H_4SiO_4 + 100%	−0.3	−0.21	−0.36
no Terr. Bio.	−0.25[d]		±0.2[e]
Observed	−0.7[f]		

[a]Sea surface values averaged 40°N–40°S, relative to results from the present-day model.
[b]Sea surface values as in footnote a but adjusted using the laboratory cultured dependence of *sacculifer* [*Spero et al*., 1999] scaled by the model-predicted change in sea surface $[CO_3^=]$.
[c]CLIMAP-2 flow field, 40×10^{15} mol terrestrial carbon at −25‰, ocean production fractionation = −18‰ [*Rau et al*., 1989].
[d]From *Leuenberger et al*. [1992].
[e]From *Marino et al*. [1992].
[f]From W. S. Broecker et al. (manuscript in preparation, 1999).

biology but generally discourage us from proposing an increase of the NO_3^- inventory that is much greater than 50% higher than today.

3.4. Ocean pH Scenarios

3.4.1. Coral reef hypothesis. A second class of pCO_2 drawdown scenarios proposes using the machinery of $CaCO_3$ compensation to change the pH of the whole ocean (Table 2). This would drive CO_2 into the ionic forms HCO_3^- and $CO_3^=$, decreasing the equilibrium pCO_2 of the atmosphere. $CaCO_3$ compensation relies on the $CO_3^=$ concentration of the deep sea to regulate the burial of $CaCO_3$ to match the rate of addition of Ca^{2+} and alkalinity to the ocean from terrestrial weathering.

One proposal for increasing ocean pH has been called the "coral reef hypothesis" [*Berger and Keir*, 1984; *Opdyke and Walker*, 1992]. $CaCO_3$ burial can be divided into two classes: deep-sea deposition, which is most sensitive to ocean pH, and shallow-water deposition, associated with reefs and tropical shelves. Deposition in shallow waters today more or less equals deep-sea deposition as a sink for $CaCO_3$ [*Milliman*, 1993]. Because sea level dropped below the depth of the continental shelves during glacial time, and because it was colder, shallow-water deposition was nearly stopped during the Last Glacial Maximum [*Kleypas*, 1997] and through stage 3 for ~50 kyr before that (J. Kleypas, personal communication, 1998). Eliminating shallow-water burial would leave a greater burial load for the deep sea, which would be accomplished in the steady state by increasing the pH of the ocean by the mechanism of $CaCO_3$ compensation.

The rate of terrestrial weathering, the other potential driver for deep-sea burial, could have been either higher or lower during glacial time. Rivers from $CaCO_3$-rich terrains are near saturation with respect to $CaCO_3$, at supersaturated CO_2 concentration, reflecting equilibrium with high CO_2 soil gas. The rate of river runoff today is much higher in the tropics than in temperate regions, so we might expect a decrease in runoff globally during the cooler glacial time [*Holland*, 1978]. On the other hand, the $CaCO_3$-rich continental shelves were exposed by lowered sea level to atmospheric weathering, and the physical abrasion of rocks by ice sheets, responsible for massive glacial deposits of finely ground glacial flour ("loess"), might have accelerated weathering [*Gibbs and Kump*, 1994; *Kump and Alley*, 1994].

3.4.1.1. Model results: The sensitivity of model pCO_2 to increasing the steady state deep-sea burial rates (equivalent to weathering) of both $CaCO_3$ and SiO_2 is given in Tables 3 and 4 and Figure 11. Increasing $CaCO_3$ burial decreases pCO_2 by increasing the pH of the ocean, and increasing the SiO_2 burial rate increases the H_4SiO_4 concentration of the ocean, decreasing the production of $CaCO_3$ and driving ocean pH still higher. We see that in the absence of a terrestrial carbon contribution, a doubling or tripling of $CaCO_3$ and SiO_2 weath-

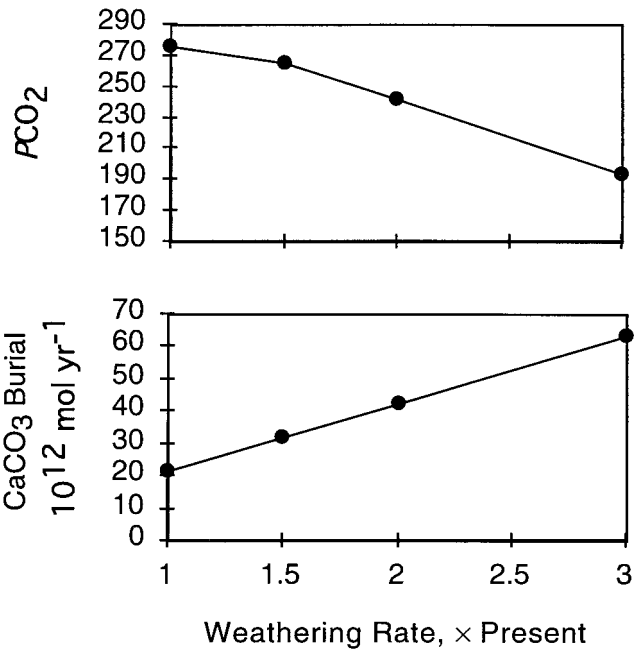

Figure 11. The pCO_2 and $CaCO_3$ sensitivity to weathering rate, after sediment compensation. These runs use the CLIMAP-2 flow field and assume the addition of 40×10^{15} mol C from the terrestrial biosphere. See also Tables 3 and 4. When the weathering rate is increased, the ocean becomes more basic in order to increase $CaCO_3$ burial, lowering pCO_2.

TABLE 6. Volume of Anoxic Waters

	Volume, 10^6 km^3
Present-day	31.9
LGM baseline	23.2
NO_3^- + 50%	53.6
NO_3^- + 100%	105.0

ering fluxes would be required to lower pCO_2 to glacial 200 μatm (Table 3). The model pCO_2 sensitivity to weathering fluxes is similar to previous results summarized by *Keir* [1995].

3.4.1.2. Paleoceanographic evidence: Several independent lines of evidence put fairly strong limits on any glacial increase in weathering intensity. Weathering tracers ^{87}Sr [*Henderson et al*., 1994] and ^{187}Os [*Oxburgh*, 1998] agree that glacial weathering rates were not significantly higher than today. *Catubig et al*. [1998] tried to estimate the glacial deep-sea burial rate of $CaCO_3$ directly from sediment accumulation data. Their analysis was limited by spotty data coverage, but they concluded that the glacial rate of deep-sea $CaCO_3$ deposition was probably not more than 50% higher than at present. This does not rule out transient changes in ocean pH that recovered too quickly to be recorded in the sediments, but the 10- to 20-kyr response time of the $CaCO_3$ concentration in surface sediments is too short to lower pCO_2 to 200 μatm for the observed interval of 50 kyr without leaving a sedimentary record. Changes in the inventory and throughflow of $CaCO_3$ may be important to understanding the transitions between glacial and interglacial states (discussed below), but they do not appear to be the primary driver for the overall glacial pCO_2 cycles.

Essentially, the mismatch between the *Catubig et al*. [1998] allowance of possible glacial deep-sea burial rate and the model requirement can be boiled down to an argument about the depth of the CCD. In order to decrease pCO_2 to glacial levels by increasing the pH of the whole ocean, we require roughly an increase in the deep-sea $[CO_3^=]$ concentration of roughly 40 μmol kg^{-1} (about a 50% increase). The pressure effect on $CaCO_3$ saturation is about 20 μmol kg^{-1} per kilometer of depth, so everything else being equal, the CCD would have moved 2 km deeper on the glacial seafloor (Figure 6e). Glacial $CaCO_3$ concentration data show the effects of rearranging the deep-ocean circulation, but it is clear that the CCD was not 2 km deeper during glacial time (Figure 6b).

3.4.2. The rain ratio model. Like the coral reef hypothesis, the rain ratio model (Table 2) [*Archer and Maier-Reimer*, 1994] proposes lowering pCO_2 by increasing the pH of the whole ocean, but this time without increasing the deep-sea $CaCO_3$ burial rate. The hope is to maintain the glacial CCD close to its present-day depth, as observed. One strategy is to decrease the production rate of $CaCO_3$, requiring a more basic ocean in order to increase the burial efficiency of $CaCO_3$. Alternatively, organic carbon, when it reacts with oxygen in sediments, produces CO_2 in the sediment pore waters, an acid which provokes $CaCO_3$ to dissolve. Therefore more organic carbon production drives more $CaCO_3$ dissolution, which also requires a higher ocean pH to compensate. *Archer and Maier-Reimer* [1994] showed that the pCO_2 is sensitive to the organic carbon and $CaCO_3$ rain rates to the seafloor by changing the fraction of organic carbon and $CaCO_3$ production which redissolves in the water column. They produced near-glacial pCO_2 by increasing organic carbon rain to the seafloor by 50% or by decreasing $CaCO_3$ rain by the same fraction. They also showed the result of decreasing the ratio of $CaCO_3$ to organic carbon produced in the surface ocean and found that a 40% decrease in $CaCO_3$ production sufficed to achieve glacial pCO_2.

The partitioning of planktonic functional types in the real ocean between $CaCO_3$ (coccolithophorids) and SiO_2 (diatoms) is only poorly understood and only crudely represented by the biological component of the ocean model. $CaCO_3$ production tends to be lower, relative to organic carbon, in productive regions, such as the Panama Basin in the eastern equatorial Pacific, and in cold places, such as the subpolar North Pacific and the Southern Ocean [*Archer*, 1996a]. Coccolithophorid production is classically thought to be associated with stratified, stagnant, nutrient-limited conditions [*Margalef*, 1978], which may have been less prevalent during glacial time. Abundant iron supply appears to favor the production of large diatoms [*Martin et al*., 1994], as does H_4SiO_4. In the future, it may be possible to resolve the upper ocean into planktonic biomes [*Longhurst*, 1998], each of which favors different functional groups of plankton (e.g., diatoms versus coccolithophorids). At present, the best we can do is a simple temperature and H_4SiO_4 supply based parameterization of $CaCO_3$ production.

The distribution of $CaCO_3$ on the seafloor today provides a feasibility test of the rain ratio mechanism. To first order, $CaCO_3$ preservation is controlled by the saturation state of the water column. If this were completely true, then the disequilibrium ($[CO_3^=] - [CO_3^=]_{saturation} = \Delta CO_3^=$) of the water column at the depth of the CCD would be everywhere the same. Variations in the rain ratio could alter the pH of the ocean by changing $\Delta CO_3^=$ at which $CaCO_3$ is preserved. If in a colder glacial world a higher organic carbon to $CaCO_3$ rain ratio drove the CCD to a higher (shallower, more saturated) $\Delta CO_3^=$, then we would expect a higher $\Delta CO_3^=$ CCD under cold places today. The maximum variation we see in the saturation state at the CCD today is about 20 μmol kg^{-1} [*Archer*, 1996a]: The CCD is at −10 μmol kg^{-1} in high latitudes but all the way down at −30 μmol kg^{-1} in the equatorial Pacific (which might still be out of steady state from the last glacial termination [*Milliman*, 1993] and hence overestimate the steady state sensitivity of the CCD $\Delta CO_3^=$ to climate above). The model is able to generate near-glacial pCO_2 by increasing deep-ocean $[CO_3^=]$ by about 20 μ*M* (by doubling H_4SiO_4; see below and Table 3), so it appears that the glacial rain ratio world would require the carbon cycle and the $\Delta CO_3^=$ at the CCD in the glacial subtropics to resemble conditions in the present-day subpolar oceans. Also, $CaCO_3$ preservation in Southern Ocean sediments is very low, implying a strong climate or H_4SiO_4 supply control on the CCD.

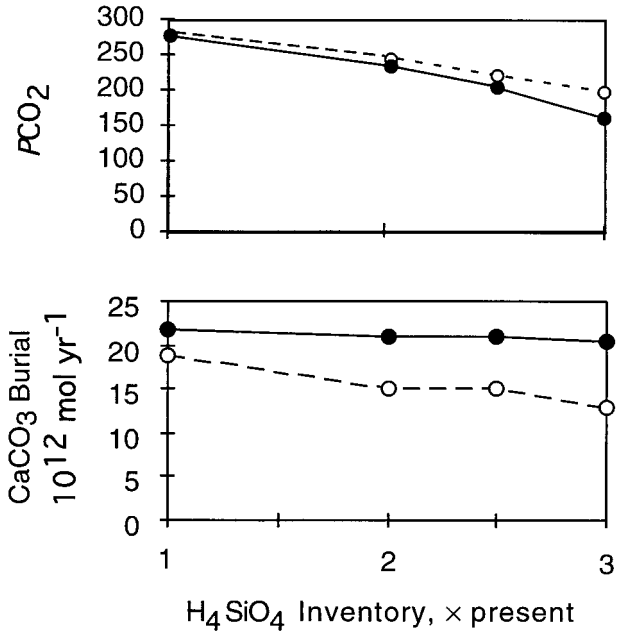

Figure 12. The pCO_2 and $CaCO_3$ sensitivity to the ocean H_4SiO_4 inventory. Open circles are uncompensated (water column steady state), and solid circles are sediment compensated for $CaCO_3$ only. The ocean inventory of H_4SiO_4 was increased as an initial condition, and H_4SiO_4 weathering rates were held equal to SiO_2 burial rates, so as to maintain the H_4SiO_4 inventory. These runs use the CLIMAP-2 flow field and assume the addition of 40×10^{15} mol carbon from the terrestrial biosphere. See Tables 3 and 4 for run details and Figure 13 for SiO_2 burial rates. We assume that increasing H_4SiO_4 would increase diatom production at the expense of $CaCO_3$ production. The decreasing alkalinity pump decreases pCO_2. Sediment compensation drives the ocean toward basic to restore $CaCO_3$ burial to the weathering rate, further decreasing pCO_2.

The model-predicted $CaCO_3$ production change based on colder glacial temperatures is relatively small, so here we test the response of the model to changes in H_4SiO_4. The ocean inventory of H_4SiO_4 is determined by the balance between influx by weathering and removal by burial. There has been a suggestion, based on the germanium to silica ratio of sedimentary diatoms, that the global rate of silica delivery to the oceans from chemical weathering might have been higher during glacial time, perhaps because of the abrasive exposure of igneous rocks by ice sheets [*Froelich et al.*, 1992]. Another possibility is that the riverine flux of H_4SiO_4 is better able to reach the ocean during glacial time because of the lack of estuaries. Currently, 5–50% of the riverine flux of H_4SiO_4 is removed from river waters in estuarine systems [*Treguer et al.*, 1995]. However, both possibilities seem to run afoul of the timing of the termination pCO_2 rise. The first asks for an increase in weathering presumably in response to the formation of ice sheets. In the termination sequence, however (Figure 2), we see pCO_2 beginning to increase while the ice sheets are still in their full glacial state. The second idea drives the H_4SiO_4 concentration of the ocean ultimately by sea level, which again gets the sequence of the transition wrong. Perhaps an increase in Si delivery to the ocean in windblown dust could be responsible.

Alternatively, it may be possible to increase ocean H_4SiO_4 by changing the sink, sedimentary burial. It has been estimated that 50–75% of the global burial of SiO_2 occurs in sediments in the "opal belt" in the Southern Ocean [*Nelson et al.*, 1995]. The high SiO_2 burial rate of the Southern Ocean is not because of extremely high rates of production but because of the episodic and punctuated nature of biological activity there [*Nelson et al.*, 1995] and perhaps because silica redissolution is slower in colder surface waters [*Hurd*, 1983]. Sinking fluxes of SiO_2 are extremely low until the conditions are right for a massive diatom bloom, which then sinks to the seafloor, delivering nearly the entire year's flux of SiO_2 to the sediment in just a few days [*Wefer et al.*, 1988]. This behavior appears to be triggered by springtime meltwater which stabilizes the upper water column, implying that Southern Ocean SiO_2 production might be sensitive to climate forcing. We have evidence that the stratification and nutrient structure in the Southern Ocean during glacial time differed from today, from isotopes of nitrogen [*Francois et al.*, 1998]. If we say that half of the SiO_2 leaves the ocean via this "Southern Ocean SiO_2 vent," then crippling this vent might decrease the global burial of SiO_2 by about a factor of 2. Under conditions of constant SiO_2 flux to the oceans the H_4SiO_4 concentration of the ocean would increase, on a timescale of 10–20 kyr, until burial everywhere else managed to make up the difference.

3.4.2.1. Model results: The pCO_2 effect of changing the model ocean concentration of H_4SiO_4 is given in Figure 12 and Table 3. The pCO_2 decreases for two reasons: a weaker biological alkalinity pump (which leaves more alkalinity in surface waters to react with CO_2), and less $CaCO_3$ rain to the seafloor (which increases ocean pH by the rain ratio mechanism). Here, in contrast to the biological pump scenarios, $CaCO_3$ compensation works in our favor, decreasing pCO_2 below levels predicted by the water-column chemistry alone. We see that an increase of a factor of 2.5 in the ocean inventory of H_4SiO_4 is required to drive pCO_2 down to glacial values, if we accept the terrestrial carbon contribution, and maybe of a factor of 2 if we decline it (see below).

However, the ocean model is unable to generate this magnitude of an ocean H_4SiO_4 increase in the steady state by any reasonable change in forcing or Southern Ocean dynamics, because the model global SiO_2 burial rate is extremely sensitive to the inventory of H_4SiO_4 in the ocean. The model SiO_2 burial rate scales with the H_4SiO_4 inventory of the ocean to the second power (Figure 13). Turn this around, and it tells us how difficult it would be to increase model ocean Si by changing weathing rates or plankton ecology. Doubling the steady state ocean H_4SiO_4 inventory by increasing weathering

would require a quadrupling of weathering. Turning off the Southern Ocean SiO_2 vent, which decreases global burial by roughly half, increases ocean H_4SiO_4 by about 40% (a factor of root 2) to compensate.

3.4.2.2. Paleoceanographic evidence: Observational support for a glacial increase in deep-ocean pH comes from boron isotopic composition of foraminifera ($CaCO_3$). The boron isotope paleo-pH meter functions as follows. Boron in seawater exists in two forms, boric acid ($B(OH)_3$) and borate ion ($B(OH)_4^-$). There is a 19‰ thermodynamic isotopic offset between the two forms, at any pH. The $\delta^{11}B$ of total boron is also independent of pH. The $\delta^{11}B$ of borate ion therefore depends on the relative proportion of borate, which is determined by pH. The idea behind the paleotracer use of boron is that only the borate form is incorporated into $CaCO_3$ shells, even (amazingly) biogenic ones [*Hemming and Hanson*, 1992; *Spivack et al*., 1993]. The relationship between $\delta^{11}B$ in $CaCO_3$ and pH has been verified by measurements of natural corals and natural and cultured foraminifera [*Sanyal et al*., 1997]. Boron pH values from the glacial deep Pacific seem to show an increase by about 0.3 pH units, which would correspond to an increase in $[CO_3^=]$ of about 100 μmol kg^{-1} [*Sanyal et al*., 1995]. This is 2.5 times higher than the $[CO_3^=]$ change produced by the 2.5 × H_4SiO_4 model and 5 times higher than that predicted by the 2 × H_4SiO_4 model with no terrestrial carbon contribution. Preliminary results from another paleo-pH tracer (sulfur in $CaCO_3$) seem to concur that glacial deep-sea pH may have been higher during glacial time [*Berry et al*., 1998].

The $\delta^{13}C$ of $CaCO_3$ from planktonic foraminifera cultured in the laboratory seem to have a pH sensitivity [*Spero et al*., 1997], as do corals [*McConnaughey*, 1989]. Benthic foraminifera have yet to be cultured as a function of pH, but if they do have a pH artifact like the planktonic species do, then perhaps the deep-ocean shift in $\delta^{13}C$ is telling us about a higher glacial deep-ocean pH rather than a smaller glacial terrestrial biosphere. If we reject the terrestrial carbon contribution and run the model with doubled H_4SiO_4, the pCO_2 decreases to 219 μatm (Table 3), and the planktonic $\delta^{13}C$, corrected for the predicted sea surface pH change, approaches observed values (Table 5). If the deep-ocean $\delta^{13}C$ really reflects a pH artifact, rather than the release of 40 × 10^{15} mol of carbon from the terrestrial biosphere, it will make explaining the low glacial pCO_2 much easier!

Another observational constraint comes from the distribution of $CaCO_3$ on the seafloor. The model of *Sigman et al*. [1998] predicts that the CCD would deepen by 1–1.5 km if tropical $CaCO_3$ production were halved (a perturbation sufficient to lower pCO_2 by 63 μatm). However, sediment cores show that the depth of the CCD was not too much different during glacial time than it is today [*Catubig et al*., 1998]. Because much of the ocean is about 4–5 km deep, and the CCD is, on average, just shallower than that, a 1.5-km deepening would vastly increase the area of high-$CaCO_3$ sediments.

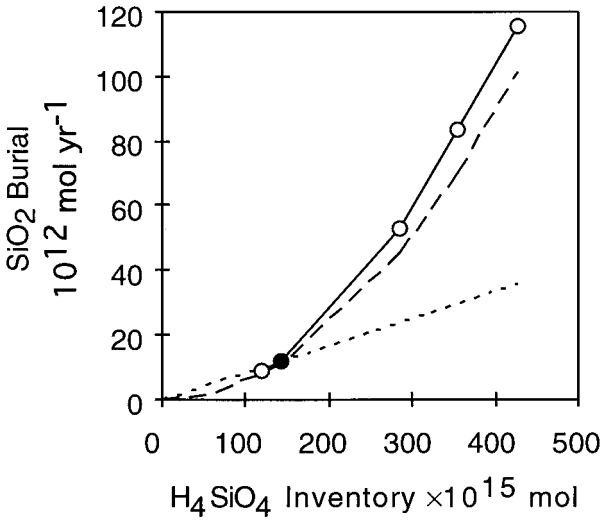

Figure 13. SiO_2 burial versus H_4SiO_4 inventory. Open circles are model results, and the solid circle is the LGM baseline case. Short-dashed line is a linear relationship between inventory and burial about the baseline case, and long-dashed line is a squared dependence (parabola) about baseline. The second-order dependence of burial on inventory implies that the inventory is only weakly (to half power) sensitive to SiO_2 weathering rate (burial).

This discrepancy was characterized as a "fatal flaw" in the rain ratio hypothesis by *Broecker and Henderson* [1998].

The distribution of $CaCO_3$ on the seafloor from the doubled H_4SiO_4 experiment is shown in Figure 6f. On average, the depth of the CCD is not radically changed, nor is the total area of $CaCO_3$ sediments. We expect qualitative differences between the *Sigman et al*. [1998] box model and the general circulation model we show here, because box models have lower pCO_2 sensitivity to tropical forcing, and lower primary production, than the circulation models do, both effects decreasing the sensitivity of pCO_2 to $CaCO_3$ production (the alkalinity pump). The change in the deep-sea $[CO_3^=]$ required to lower pCO_2 is smaller in the doubled H_4SiO_4 model here than in the *Sigman et al*. [1998] model, 20 μ*M* versus 40 μ*M*, halving the expected excursion of the CCD depth. The deepening CCD effect that *Sigman et al*. [1998] identify was also evident in the *Archer and Maier-Reimer* [1994] model, when the ratio of $CaCO_3$ to organic C production was changed in a spatially uniform way (unpublished results), but is less obvious here, perhaps because the changes in $CaCO_3$ production provoked by doubling H_4SiO_4 are spatially nonuniform. The fatal flaw in the rain ratio hypothesis seems less clear than it did from the *Sigman et al*. [1998] model.

In the real glacial ocean the CCD in the Atlantic shoaled, while calcite was preserved at greater depths in the Pacific [*Berger*, 1973; *Broecker and Peng*, 1982; *Broecker*, 1993a]. The model predicts the opposite response to doubling H_4SiO_4, because H_4SiO_4 is concentrated in the glacial model Pacific, as it is today, so increasing

H_4SiO_4 has a greater impact on the rain ratio in the Pacific. However, we have little confidence in the near-surface distribution of H_4SiO_4 in the model because glacial Pacific intermediate water in the real ocean was more ventilated than it is today [*Kennett and Ingram*, 1995], a feature which is missed by the model. $CaCO_3$-depleted sediments in the model occur under upwelling areas such as the equatorial Pacific, where abundant H_4SiO_4 supply precludes much production of $CaCO_3$, while in reality $CaCO_3$ concentration and accumulation increased sharply in this region [*Farrell and Prell*, 1989]. In short, the model-predicted distribution of $CaCO_3$ on the seafloor is a poor fit to observations (Figure 6). If the rain ratio hypothesis is the correct one, our glacial circulation field and crude biology model are doing a poor job of simulating the glacial distribution of $CaCO_3$ production.

Another test of whole-ocean pH change scenarios may come from the magnitude of $CaCO_3$ preservation anomalies at the glacial transitions as the ocean adjusts its chemistry from glacial to interglacial conditions. Sediment cores often show high $CaCO_3$ preservation on deglacial transitions and a "dissolution spike" on the transitions to glacial periods [*Peterson and Prell*, 1985]. The terrestrial carbon contribution to the glacial ocean, when it was withdrawn at the glacial termination, would have required the precipitation of about 40×10^{15} mol of $CaCO_3$ to restore the pH of the ocean. If we spread the anomaly over 10 kyr, we would produce a burial rate anomaly of 4×10^{12} mol yr^{-1}, which is significant relative to the present-day burial rate of about 12×10^{12} mol yr^{-1} of $CaCO_3$. $CaCO_3$ accumulation in shallow-water sediments and coral reefs began to increase as the continental shelves flooded, to a rate of $10–15 \times 10^{12}$ mol yr^{-1} [*Milliman*, 1993; *Kleypas*, 1997], which would tend to provoke a deep-sea accumulation rate anomaly of perhaps $-100–150 \times 10^{15}$ mol (negative denotes dissolution). The whole-ocean pH change required by a rain ratio model would generate a large $CaCO_3$ burial anomaly of $+150 \times 10^{15}$ mol of $CaCO_3$, at a rate of $+15 \times 10^{12}$ mol yr^{-1} over the 10-kyr timescale of the pCO_2 transition. A wild card in the mix is the rate of weathering, which might have peaked as patterns of rainfall changed at the climate transition (although tracers indicate not [*Oxburgh*, 1998]); another complication is the possibility that the global ocean appears to be out of $CaCO_3$ weathering/burial steady state today [*Milliman*, 1993]. The magnitude of the termination $CaCO_3$ burial anomaly has not yet been estimated, but we note that the simplest case, which includes the terrestrial carbon contribution, termination onset of shallow-water deposition, and constant weathering fluxes, predicts a termination dissolution spike, not a preservation spike as observed. We require either a weathering transient, or a whole-ocean pH shift, or an uncoupling in time (first terrestrial carbon, then coral reefs) to generate a $CaCO_3$ preservation spike at the glacial termination as observed. Evidence from earlier climate transitions is elusive because our dating tool, ^{14}C, has decayed away, but a dissolution spike at the previous glaciation dated using cosmic dust ^3He appeared to be of the right magnitude to accommodate a whole-ocean pH change [*Broecker and Sanyal*, 1997].

4. CONCLUSIONS

Many constraints on the cause of the glacial/interglacial atmospheric pCO_2 come from ice core and sedimentary records. First, the deglacial increase in pCO_2 leads ice volume, eliminating sea-level-driven explanations such as those based on the submersion of the continental shelves [*Sowers and Bender*, 1995; *Broecker and Henderson*, 1998]. Second, the deglacial pCO_2 transition was slow: 6–7 kyr in one case and as much as 14 kyr in the other. The pCO_2 response time to the biological pump in the ocean is much faster than that, and so biological pump explanations would require some external pacer to slow the pCO_2 transition. Third, the glacial rate of weathering and global deep-sea $CaCO_3$ burial was probably not much higher than today [*Henderson et al*., 1994; *Catubig et al*., 1998; *Oxburgh*, 1998]. Additional constraints come from isotopic signatures of carbon, nitrogen, and boron, the concentrations of the trace metal species cadmium and barium, and the distribution of $CaCO_3$ and SiO_2 on the seafloor.

The ingredients of the glacial ocean that control CO_2, simulated to the best of our knowledge in a numerical model, are as follows:

1. The first is the circulation of the ocean. The direct effect of the glacial circulation and surface ocean cooling on pCO_2 appears to be small, especially after $CaCO_3$ compensation.

2. The second is iron fertilization. Even if sea surface nutrients were completely depleted by a stronger biological cycle in the ocean (a much stronger response than is inferred for the glacial ocean), pCO_2 would not reach the glacial concentration of 200 μatm, especially if we release 40×10^{15} mol C from the terrestrial biosphere. Perhaps this is an artifact of excessive diapycnal diffusion in the z-coordinate circulation model.

3. The third is sediment geochemistry. Changes in biological production and water chemistry affect the diagenesis and burial of $CaCO_3$, and hence pCO_2. A new sediment model is able to simulate the transition to anaerobic conditions, efficiently enough to implement at every grid point in a global ocean model. The most striking effect of the anaerobic chemistry is to greatly enhance $CaCO_3$ burial with decreasing oxygen concentration in the deep sea. This effect drives $CaCO_3$ compensation to completely override the pCO_2 drawdown from a proposed increase in ocean nutrients.

Three possibilities emerge as front-runners to address the discrepancy between observations and our present state of knowledge, although none of them fit the data

well. The first is that the ocean circulation models now in use for simulating the ocean carbon cycle are more diffusive than the real ocean and for this reason underestimate the pCO_2 sensitivity to the biological pump. The verdict on this possibility awaits reconciliation of a suite of discordant field and modeling estimates of diffusivity in the real ocean [*Archer et al.*, 2000]. The second possibility is to increase the glacial NO_3^- inventory of the ocean beyond PO_4^{3-} limitation. Here we would assume that the Redfield ratio of N/P in phytoplankton was different during glacial time. This hypothesis is consistent with carbon isotopic data but generates anoxic conditions in the Pacific thermocline and a general decrease in the oxygen content of the deep sea as a whole. Decreasing oxygen in turn promotes $CaCO_3$ burial, requiring an eventual decrease in ocean pH to compensate, which raises pCO_2. Perhaps a source of ventilation to the intermediate Pacific [*Kennett and Ingram*, 1995], missed by our adjoint fit to the glacial ocean circulation, could alleviate some of these coupled problems. The third possibility is to double the inventory of H_4SiO_4 in the ocean, thereby shifting the ratio of organic carbon to $CaCO_3$ production and raising the pH of the deep ocean. This hypothesis is consistent with boron isotopes (a paleo-pH tracer), and if a benthic pH artifact on $\delta^{13}C$ is found such as has been found for planktonic foraminifera, then this scenario might be consistent with carbon isotope data as well. However, the predicted distribution of $CaCO_3$ is not a good match for observations. Here the difficulty is explaining why the ocean H_4SiO_4 should have increased; the model global SiO_2 burial rate scales with the H_4SiO_4 inventory squared, implying that H_4SiO_4 is relatively insensitive to SiO_2 weathering or details of burial mechanism. Perhaps the dynamics of SiO_2 production in surface waters and dissolution in sediments is not captured by the model.

We conclude that in spite of the importance of understanding the natural carbon cycle, the solution to the mystery of the glacial/interglacial CO_2 cycles still eludes us.

APPENDIX 1: PARAMETERIZATION OF BIOLOGICAL PRODUCTIVITY

In iron- and light-saturated conditions the maximum rate of PO_4^{3-} uptake in the surface ocean is given by

$$R_{\mathrm{PO_4max}} = Pr_{\mathrm{lat}} \times \mathrm{PO_4} \times \frac{\mathrm{PO_4}}{\mathrm{PO_4} + P_{\mathrm{half\text{-}sat}}},$$

where PO_4 is the nutrient concentration, $P_{\mathrm{half\text{-}sat}}$ is a half-saturation constant, here equal to 0.0001 μM, and Pr_{lat} is a latitude-dependent light limitation factor, which varies smoothly from 1.0 at the equator to 0.5 in the Southern Ocean. $P_{\mathrm{half\text{-}sat}}$ is a very small number, enabling complete nutrient uptake where iron and light conditions permit. The maximum uptake of upwelled dissolved iron is estimated similarly,

$$R_{\mathrm{Fe_{max}}} = \mathrm{Fe} \times \frac{\mathrm{Fe}}{\mathrm{Fe} + \mathrm{Fe_{half\text{-}sat}}},$$

where $Fe_{\mathrm{half\text{-}sat}}$ is taken to be 0.003 nM, another small number. Total carbon export is taken to be the minimum of

$$R_{\mathrm{orgC}} = \min\left(106 \times R_{\mathrm{PO_4max}}, 2 \times 10^5 \times Pr_{\mathrm{lat}} \times (R_{\mathrm{Fe_{max}}} + \mathrm{Atm_{Fe}})\right) \quad (1)$$

where Atm_{Fe} is the atmospheric deposition rate of iron. The application of the light limitation factor Pr_{lat} to the iron field decreases the impact of Southern Ocean dust on annual mean sea surface PO_4^{3-} concentration. Without light limitation it was impossible to reproduce the high sea surface nutrient concentrations in the North Pacific (a region of high dust fluxes) and to differentiate the Southern Ocean from the South Pacific (both regions of low dust) [*Archer and Johnson*, 2000].

Iron-unlimited (maximum) uptake of H_4SiO_4 is parameterized as

$$R_{\mathrm{H_4SiO_4max}} = Pr_{\mathrm{lat}} \times \mathrm{H_4SiO_4} \times \frac{\mathrm{H_4SiO_4}}{\mathrm{H_4SiO_4} + \mathrm{Si_{half\text{-}sat}}},$$

where $Si_{\mathrm{half\text{-}sat}}$ is taken to be 4 μM. Iron limitation takes the form of (1), above. Production of $CaCO_3$ is taken to be

$$R_{\mathrm{CaCO_3}} = 0.305 \times (R_{\mathrm{orgC}} - 1.0 \times R_{\mathrm{Si}}) \times \frac{T_{\mathrm{fac}}}{5 + T_{\mathrm{fac}}},$$

with T_{fac} is defined as $T_{\mathrm{fac}} = e^{T-3.5}$, where T is temperature.

APPENDIX 2: SEDIMENTARY MODEL FORMULATION AND NUMERICAL METHOD

The "Muds" diagenetic model for organic carbon, oxygen, nitrate, iron, manganese, and sulfides is based on the steady state diffusion/reaction equations for pore water and sediments. The model equations and Monod reaction kinetics are similar to previously published sedimentary diagenetic models [*Burdige and Geiskes*, 1983; *Archer*, 1991; *van Cappellen and Wang*, 1996]. Two types of organic carbon, one more reactive than the other, rain to the seafloor and react initially with O_2 in the pore waters [*Berner*, 1980b]. NO_3^- serves as an electron acceptor below the depth where O_2 is depleted. In this zone, solid MnO_2 is also used as an electron acceptor for respiration, producing dissolved Mn^{2+}, which diffuses to the oxic zone and reprecipitates. Below the depth where NO_3^- is depleted, solid iron oxides are used as an electron acceptor, producing dissolved Fe^{2+}, which either reacts with H_2S to form iron sulfides or diffuses upward to the oxic zone and precipitates similarly to Mn.

The equation for a pore water solute concentration, c, is

TABLE A1. Sedimentary Model Reactions and Rate Expressions

Reaction	*k*	*Rate*,[a] *mol* L^{-1} s^{-1}
Fast OrgC + $138O_2 \rightarrow 106CO_2 + 16NO_3^-$	1.0×10^{-7}	$k \times$ [Fast OrgC][b]
Slow OrgC + $138O_2 \rightarrow 106CO_2 + 16NO_3^-$	5.0×10^{-10}	$k \times$ [Slow OrgC]
$Mn^{2+} + 1/2O_2 + H_2O \rightarrow MnO_2 + 2H^+$	5.0×10^{-7}	$k \times [Mn^{2+}]$[c]
OrgC + $236MnO_2 + 472H^+ \rightarrow 236Mn^{2+} + 106CO_2 + 16NO_3^-$	1.0×10^{-7}	$k \times$ [OrgC] $\times$ $[MnO_2]$[d]
OrgC + $94.4HNO_3 \rightarrow 106CO_2 + 47.2N_2$	2.0×10^{-11}	$k \times$ [OrgC]
$Fe^{2+} + 1/2O_2 \rightarrow FeOOH + H^+$	1.0×10^{-8}	$k \times [Fe^{2+}]$[c]
OrgC + $472FeOOH + 944H^+ \rightarrow 106CO_2 + 472Fe^{2+} + 8N_2$	1.0×10^{-10}	$k \times$ [OrgC] $\times$ [FeOOH][e]
OrgC + $59SO_4^{2-} + 59H^+ \rightarrow 106CO_2 + 8N_2 + 59HS^-$	1.0×10^{-13}	$k \times$ [OrgC][e]
$HS^- + 2O_2 \rightarrow SO_4^{2-} + H^+$	1.0×10^{-6}	k[c,f]
$HS^- + FE^{2+} \rightarrow FeS + H^+$	instantaneous	no coexistence of HS^- and Fe^{2+} is allowed
$FeS + 4.5O_2 + H^+ \rightarrow FeOOH + SO_4^{2-}$	1.0×10^{-9}	$k \times [FeS] \times O_2$
$CaCO_3 \rightarrow Ca^{2+} + CO_3^-$	1.0×10^{-3}	$k \times [1 - [CO_3^=]/[CO_3^=]_{sat})$
$SiO_2 \rightarrow H_4SiO_4$	7.5×10^{-6}	$k \times [SiO_2] \times ([H_4SiO_4]_{sat} - [H_4SiO_4])$

[a]Units of mol L^{-1} s^{-1}.
[b]OrgC denotes organic carbon with stoichiometry $(CH_2O)_{106}(NH_3)_{16}$.
[c]In the presence of dissolved O_2.
[d]In the absence of dissolved O_2.
[e]In the absence of dissolved NO_3^-.
[f]In the presence of HS^-.

$$\phi \frac{\partial c}{\partial t} = 0 = \frac{\partial}{\partial z}\left(\frac{D_c}{F}\frac{\partial c}{\partial z}\right) - R_c,$$

where ϕ is the sediment porosity, D_c is the diffusion coefficient for that solute, F is the formation factor of the sediment which describes the attenuation of diffusion by the solid matrix, z is depth (positive downward), and R_c is the reaction rate, given for each of the solutes in Table A1.

Transport of solid species is governed by the equation

$$(1 - \phi)\frac{\partial \%S}{\partial t} = 0 = D_B \frac{\partial}{\partial z}\left[(1 - \phi)\frac{\partial \%S}{\partial z}\right] - R_S,$$

where D_B is the solid diffusion (bioturbation) rate, which is assumed to decrease exponentially over a scale depth of 10 cm. By setting the time-dependent term equal to zero, we solve for the steady state profile of organic carbon, which should establish itself in nature on a timescale of the order of hundreds of years.

The novelty of the Muds sediment model is the numerical method, which converges directly to the steady state profiles of solutes and solids. This method is orders of magnitude faster than can be achieved by integrating the time-dependent equations forward until they reach steady state (the more common method) and affords us the opportunity to couple the sediment code to each grid cell of the global ocean model. From an initial guess of the concentrations of each species at each depth, the model relies on the derivatives of the fluxes in each grid cell by the concentrations to formulate a next iteration, analogously to Newton's method for finding the zero to a function by projecting a tangent of the function toward the desired result to generate a next guess. Typically, the full solution, determined as flux balance for each solid and dissolved constituent within a tolerance of 1%, emerges after 100–200 iterations. For the solutes, diffusive fluxes into a cell depend on the concentrations above and below the cell, as well as on the cell concentration itself. Therefore iterations on the solute profiles proceed simultaneously for a single solute over the entire model domain (all the grid cells over depth). Solute and solid concentrations are coupled together in a variety of complicated ways. Solid concentrations determine or at least influence the reaction rates, which determine solute profiles and further feed back to reaction rates. The reaction rates, in turn, determine the profile of sediment burial (advection) fluxes, which further feeds back to the solid concentration profiles of all solid species and thence to the rest of the solutes. Rather than attempt to treat all of the solid and solute concentration profiles simultaneously, the model iterates between solutes and solids by incrementally guessing solid concentrations, then calculating the resulting steady state solute profiles, back and forth.

ACKNOWLEDGMENTS. This paper benefited from sabbatical support of David Lea at the University of Chicago, from ongoing discussion with Wally Broecker, and from terrific editorial input by Tom Torgersen.

Thomas Torgerson was the Editor responsible for this paper. He thanks Robin Kier and an anonymous reviewer for their help in evaluating this paper.

REFERENCES

Altabet, M. A., and W. B. Curry, Testing models of past ocean chemistry using foraminifera $^{15}N/^{14}N$, *Global Biogeochem. Cycles*, *3*, 107–119, 1989.

Altabet, M. A., and R. Francois, Sedimentary nitrogen isotopic ratio as a recorder for surface ocean nitrate utilization, *Global Biogeochem. Cycles*, *8*, 103–116, 1994.

Altabet, M. A., R. Francois, D. W. Murray, and W. L. Prell, Climate-related variations in denitrification in the Arabian Sea from sediment $^{15}N/^{14}N$ ratios, *Nature*, *373*, 506–509, 1995.

Archer, D. E., Modeling the calcite lysocline, *J. Geophys. Res.*, *96*, 17,037–17,050, 1991.

Archer, D. E., An atlas of the distribution of calcium carbonate in sediments of the deep sea, *Global Biogeochem. Cycles*, *10*, 159–174, 1996a.

Archer, D. E., A data-driven model of the global calcite lysocline, *Global Biogeochem. Cycles*, *10*, 511–526, 1996b.

Archer, D. E., and K. Johnson, A model of the iron cycle in the ocean, *Global Biogeochem. Cycles*, *14*, 269–279, 2000.

Archer, D. E., and E. Maier-Reimer, Effect of deep-sea sedimentary calcite preservation on atmospheric CO_2 concentration, *Nature*, *367*, 260–264, 1994.

Archer, D., M. Lyle, K. Rodgers, and P. Froelich, What controls opal preservation in tropical deep-sea sediments, *Paleoceanography*, *8*, 7–21, 1993.

Archer, D., H. Kheshgi, and E. Maier-Riemer, Multiple timescales for neutralization of fossil fuel CO_2, *Geophys. Res. Lett.*, *24*, 405–408, 1997.

Archer, D. E., G. Eshel, A. Winguth, W. Broecker, R. Pierrehumbert, M. Tobis, and R. Jacob, Atmospheric pCO_2 sensitivity of ocean/atmosphere carbon cycles, *Global Biogeochem. Cycles*, in press, 2000.

Bacastow, R. B., The effect of temperature change of the warm surface waters of the oceans on atmospheric CO_2, *Global Biogeochem. Cycles*, *10*, 319–333, 1996.

Bard, E., F. Rostek, and C. Sonzogni, Interhemispheric synchrony of the last deglaciation inferred from alkenone paleothermotry, *Nature*, *385*, 707–710, 1997.

Berger, W. H., Deep-sea carbonates: Pleistocene dissolution cycles, *J. Foraminiferal Res.*, *3*(4), 187–195, 1973.

Berger, W. H., Deglacial CO_2 buildup: Constraints on the coral reef model, *Palaeogeogr. Palaeoclimatol. Palaeoecol.*, *40*, 235–253, 1982.

Berger, W. H., and R. S. Keir, Glacial-Holocene changes in atmospheric CO_2 and the deep-sea record, in *Climate Processes and Climate Sensitivity*, *Geophys. Monogr. Ser.*, vol. 29, edited by J. E. Hansen and T. Takahashi, pp. 337–351, AGU, Washington, D. C., 1984.

Berner, R. A., *Early Diagenesis: A Theoretical Approach*, Princeton Univ. Press, Princeton, N. J., 1980a.

Berner, R. A., A rate model for organic matter decomposition during bacterial sulfate reduction in marine sediments, in *Biogeochemistry of Organic Matter at the Sediment-Water Interface*, edited by R. Doumas, Comm. Natl. Rech. Sci., Paris, 1980b.

Berner, R. A., A. C. Lasaga, and R. M. Garrels, The carbonate-silicate geochemical cycle and its effect on atmospheric carbon dioxide over the past 100 million years, *Am. J. Sci.*, *283*, 641–683, 1983.

Berry, J. N., E. A. Boyle, and J. Erez, Investigating sulfur in foraminiferal calcite as a potential seawater pH proxy, *Eos Trans. AGU*, *79*(17), Spring Meet. Suppl., S181, 1998.

Betzer, P. R., R. H. Byrne, J. G. Acker, C. S. Lewis, and R. R. Jolley, The oceanic carbonate system: A reassessment of biogenic controls, *Science*, *226*, 1074–1077, 1984.

Boyle, E. A., Cadmium: Chemical tracer of deepwater paleoceanography, *Paleoceanography*, *3*, 471–489, 1988a.

Boyle, E. A., Vertical oceanic nutrient fractionation and glacial/interglacial CO_2 cycles, *Nature*, *331*, 55–56, 1988b.

Boyle, E. A., Cadmium and $\delta^{13}C$ paleochemical ocean distributions during the Stage 2 glacial maximum, *Annu. Rev. Earth Planet. Sci.*, *20*, 245–287, 1992.

Brand, L. E., Minimum iron requirements of marine phytoplankton and the implications for biogeochemical control of new production, *Limnol. Oceanogr.*, *36*, 1756–1771, 1991.

Brandes, J. A., and A. H. Devol, Isotopic fractionation of oxygen and nitrogen in coastal marine sediments, *Geochim. Cosmochim. Acta*, *61*, 1793–1801, 1997.

Broecker, W. S., Glacial to interglacial changes in ocean chemistry, *Prog. Oceanogr.*, *11*, 151–197, 1982a.

Broecker, W. S., Ocean chemistry during glacial time, *Geochim. Cosmochim. Acta*, *46*, 1689–1705, 1982b.

Broecker, W. S., *The Glacial World According to Wally*, Lamont-Doherty Earth Obs., Palisades, N. Y., 1993a.

Broecker, W. S., An oceanographic explanation for the apparent carbon isotope-cadmium discordancy in the glacial Antarctic?, *Paleoceanography*, *8*, 137–139, 1993b.

Broecker, W. S., and G. Henderson, The sequence of events surrounding Termination II and their implications for the cause of glacial-interglacial CO_2 changes, *Paleoceanography*, *13*, 352–364, 1998.

Broecker, W. S., and E. Maier-Reimer, The influence of air and sea exchange on the carbon isotope distribution in the sea, *Global Biogeochem. Cycles*, *6*, 315–320, 1992.

Broecker, W. S., and T.-H. Peng, *Tracers in the Sea*, Lamont-Doherty Earth Obs., Palisades, N. Y., 1982.

Broecker, W. S., and T.-H. Peng, The role of $CaCO_3$ compensation in the glacial to interglacial atmospheric CO_2 change, *Global Biogeochem. Cycles*, *1*, 15–29, 1987.

Broecker, W. S., and A. Sanyal, Magnitude of the $CaCO_3$ dissolution events marking the onset of times of glaciation, *Paleoceanography*, *12*, 530–532, 1997.

Broecker, W. S., and T. Takahashi, The relationship between lysocline depth and in situ carbonate ion concentration, *Deep Sea Res.*, *25*, 65, 1978.

Broecker, W., J. Lynch-Steiglitz, D. Archer, M. Hofmann, E. Maier-Reimer, O. Marchal, T. Stocker, and N. Gruber, How strong is the Harvardton-Bear constraint?, *Global Biogeochem. Cycles*, *13*, 817–820, 1999.

Burdige, D., and J. M. Geiskes, A pore water/solid phase diagenetic model for manganese in marine sediments, *Am. J. Sci.*, *283*, 29–47, 1983.

Canfield, D. E., Sulfate reduction and oxic respiration in marine sediments: Implications for organic carbon preservation in euxinic environments, *Deep Sea Res.*, *36*, 121–138, 1989.

Capone, D. G., J. P. Zehr, H. W. Paerl, B. Bergman, and E. J. Carpenter, Trichodesmium: A globally significant marine cyanobacterium, *Science*, *276*, 1221–1229, 1997.

Catubig, N., D. E. Archer, R. Francois, P. deMenocal, W. Howard, and E.-F. Yu, Global deep-sea burial rate of calcium carbonate during the Last Glacial Maximum, *Paleoceanography*, *13*, 298–310, 1998.

Charles, C. D., J. D. Wright, and R. G. Fairbanks, Thermodynamic influences on the marine carbon isotope record, *Paleoceanography*, *8*, 691–697, 1993.

CLIMAP Project Members, Seasonal reconstruction of the Earth's surface at the Last Glacial Maximum, *Geol. Soc. Am. Map Chart Ser.*, *MC-36*, 1981.

Coale, K. H., et al., A massive phytoplankton bloom induced by an ecosystem-scale iron fertilization experiment in the equatorial Pacific Ocean, *Nature*, *383*, 495–501, 1996.

Cochran, J. K., and S. Krishnaswami, Radium, thorium, uranium and 210 Pb in deep-sea sediments and sediment pore waters from the north equatorial Pacific, *Am. J. Sci.*, *280*, 849–889, 1980.

Crowley, T. J., Ice age terrestrial carbon changes revisited, *Global Biogeochem. Cycles*, *9*, 377–389, 1995.

Curry, W. B., and G. P. Lohmann, Carbon isotope changes in benthic foraminifera from the western South Atlantic: Reconstruction of glacial abyssal circulation patterns, *Quat. Res.*, *18*, 218–235, 1982.

Curry, W. B., J. C. Duplessy, L. D. Labeyrie, and N. J. Shackleton, Changes in the distribution of $\delta^{13}C$ of deep ΣCO_2

between the last glaciation and the Holocene, *Paleoceanography*, *3*, 317–341, 1988.

Duce, R. A., and N. W. Tindale, Atmospheric transport of iron and its deposition in the ocean, *Limnol. Oceanogr.*, *36*, 1715–1726, 1991.

Dugdale, R. C., and J. J. Goering, Uptake of new and regenerated forms of nitrogen in primary productivity, *Limnol. Oceanogr.*, *12*, 196–207, 1967.

Duplessy, J. C., N. J. Shackleton, R. G. Fairbanks, L. Labeyrie, D. Oppo, and N. Kallel, Deepwater source variations during the last climatic cycle and their impact on the global deepwater circulation, *Paleoceanography*, *3*, 343–360, 1988.

Elser, J. J., and R. P. Hassett, A stoiciometric analysis of the zooplankton-phytoplankton interaction in marine and freshwater ecosystems, *Nature*, *370*, 211–213, 1994.

Emerson, S., and M. L. Bender, Carbon fluxes at the sediment-water interface of the deep sea: Calcium carbonate preservation, *J. Mar. Res.*, *39*, 139–162, 1981.

Emerson, S., P. Quay, D. Karl, C. Winn, L. Tupas, and M. Landry, Experimental determination of the organic carbon flux from open-ocean surface waters, *Nature*, *389*, 951–954, 1997.

Fairbanks, R. G., A 17,000 year glacio-eustatic sea level record: Influence of glacial melting rates on the Younger Dryas event and deep-ocean circulation, *Nature*, *143*, 637–642, 1989.

Falkowski, P. G., Evolution of the nitrogen cycle and its influence on the biological sequestration of CO_2 in the ocean, *Nature*, *387*, 272–274, 1997.

Fanning, K. A., Nutrient provinces in the sea: Concentration ratios, reaction rate ratios, and ideal covariation, *J. Geophys. Res.*, *97*, 5693–5712, 1992.

Farrell, J. W., and W. L. Prell, Climate change and $CaCO_3$ preservation: An 800,000-year bathymetric reconstruction from the central equatorial Pacific Ocean, *Paleoceanography*, *4*, 447–466, 1989.

Farrell, J. W., T. F. Pederson, S. E. Calvert, and S. E. Nielsen, Glacial-interglacial changes in nutrient utilization in the equatorial Pacific Ocean, *Nature*, *377*, 514–517, 1995.

Francois, R., M. A. Altabet, E.-F. Yu, D. M. Sigman, M. P. Bacon, M. Frank, G. Bohrmann, G. Bareille, and L. D. Labeyrie, Contribution of Southern Ocean surface-water stratification to low atmospheric CO_2 concentration during the last glacial period, *Nature*, *389*, 929–936, 1998.

Froelich, P. N., et al., Early oxidation of organic matter in pelagic sediments of the eastern equatorial Atlantic: Suboxic diagenesis, *Geochim. Cosmochim. Acta*, *43*, 1075–1090, 1979.

Froelich, P. N., M. L. Bender, N. A. Luedtke, G. R. Heath, and T. DeVries, The marine phosphorus cycle, *Am. J. Sci.*, *282*, 474–511, 1982.

Froelich, P. N., V. Blanc, R. A. Mortlock, S. N. Chillrud, W. Dunstan, A. Udomkit, and T.-H. Peng, River fluxes of dissolved silica to the ocean were higher during glacials: Ge/Si in diatoms, rivers, and oceans, *Paleoceanography*, *7*, 739–767, 1992.

Ganeshram, R. S., T. F. Pedersen, S. E. Calvert, and J. W. Murray, Large changes in oceanic nutrient inventories from glacial to interglacial periods, *Nature*, *376*, 755–758, 1995.

Gargett, A. E., and G. Holloway, Dissipation and diffusion by internal wave breaking, *J. Mar. Res.*, *42*, 15–27, 1984.

Gibbs, M., and L. R. Kump, Global chemical erosion during the Last Glacial Maximum and the present: Sensitivity to changes in lithology and hydrology, *Paleoceanography*, *9*, 529–543, 1994.

Gnanadesikan, A., A global model of silicon cycling: Sensitivity to eddy parameterization and dissolution, *Global Biogeochem. Cycles*, *13*, 199–220, 1999.

Goldman, J. C., Oceanic nutrient cycles, in *Flows of Energy and Materials in Marine Ecosystems: Theory and Practice*, edited by M. J. R. Fasham, pp. 137–170, Plenum, New York, 1984.

Gruber, N., and J. L. Sarmiento, Global patterns of marine nitrogen fixation and denitrification, *Global Biogeochem. Cycles*, *11*, 235–266, 1997.

Guilderson, T. P., R. G. Fairbanks, and J. L. Rubinstone, Tropical temperature variations since 20,000 years ago: Modulating interhemispheric climate change, *Science*, *263*, 663–665, 1994.

Hays, J. D., J. Imbrie, and N. J. Shackleton, Variations in the Earth's orbit: Pacemaker of the ice ages, *Science*, *194*, 1121–1132, 1976.

Hecky, R. E., E. P. Campbell, and L. L. Hendzel, The stoiciometry of carbon, nitrogen, and phosphorus in particulate matter of lakes and oceans, *Limnol. Oceanogr.*, *38*, 709–724, 1993.

Heinze, C., and W. S. Broecker, Closing off the Southern Ocean surface, *Paleoceanography*, *10*, 49–58, 1995.

Heinze, C., E. Maier-Reimer, and K. Winn, Glacial pCO_2 reduction by the world ocean: Experiments with the Hamburg carbon cycle model, *Paleoceanography*, *6*, 395–430, 1991.

Heinze, C., E. Maier-Reimer, A. M. E. Winguth, and D. Archer, A global oceanic sediment model for long-term climate studies, *Global Biogeochem. Cycles*, *13*, 221–250, 1999.

Hemming, N. G., and G. N. Hanson, Boron isotopic composition and concentration in modern marine carbonates, *Geochim. Cosmochim. Acta*, *56*, 537–544, 1992.

Henderson, G. M., D. J. Martel, R. K. O'Nions, and N. J. Shackleton, Evolution of seawater 87Sr/87Sr over the last 400 ka: The absence of glacial/interglacial cycles, *Earth Planet. Sci. Lett.*, *128*, 643–651, 1994.

Holland, H. D., *The Chemistry of the Atmosphere and Oceans*, John Wiley, New York, 1978.

Hu, D., A joint mixed-layer/isopycnic coordinate numerical model of wind- and thermohaline-driven ocean general circulation with model sensitivity study, Ph.D. thesis, Univ. of Miami, Miami, Fla., 1991.

Hu, D., On the sensitivity of thermocline depth and meridional heat transport to vertical diffusivity in OGCM's, *J. Phys. Oceanogr.*, *26*, 1480–1494, 1996.

Hurd, D. C., *Physical and Chemical Properties of Siliceous Skeletons*, Academic, San Diego, Calif., 1983.

Hurd, D. C., C. Fraley, and J. K. Fugate, Silica apparent solubilities and rates of dissolution and precipitation; for ca. 25 common minerals at 1–2 degrees C, pH 7.5–8.5 in seawater, in *Chemical Modeling in Aqueous Systems: Speciation, Sorption, Solubility, and Kinetics*, edited by E. A. Jenne, pp. 413–446, *ACS Symp. Ser.*, vol. 93, U.S. Geol. Surv., Menlo Park, Calif., 1979.

Imbrie, J., et al., On the structure and origin of major glaciation cycles, 1, Linear responses to Milankovitch forcing, *Paleoceanography*, *7*, 701–738, 1992.

Imbrie, J., et al., On the structure and origin of major glaciation cycles, 2, The 100,000-year cycle, *Paleoceanography*, *8*, 699–735, 1993.

Jenkins, W. J., Nitrate flux into the euphotic zone near Bermuda, *Nature*, *331*, 521–524, 1988.

Jenkins, W. J., and D. W. R. Wallace, Tracer based inferences of new primary production in the sea, in *Primary Productivity and Biogeochemical Cycles in the Sea*, edited by P. G. Falkowski and A. D. Woodhead, pp. 299–316, Plenum, New York, 1992.

Johnson, K. S., R. M. Gordon, and K. H. Coale, What controls dissolved iron concentrations in the world ocean?, *Mar. Chem.*, *57*, 137–161, 1997.

Joos, F., J. C. Orr, and U. Siegenthaler, Ocean carbon trans-

port in a box-diffusion versus a general circulation model, *J. Geophys. Res*., *102*, 12,367–12,388, 1997.
Keigwin, L. D., Glacial-age hydrography of the far northwest Pacific Ocean, *Paleoceanography*, *13*, 323–339, 1998.
Keir, R. S., On the late Pleistocene ocean geochemistry and circulation, *Paleoceanography*, *3*, 413–445, 1988.
Keir, R. S., Is there a component of Pleistocene CO_2 change associated with carbonate dissolution cycles?, *Paleoceanography*, *10*, 871–880, 1995.
Kennett, J., and B. Ingram, A 20,000-year record of ocean circulation and climate change from the Santa Barbara basin, *Nature*, *377*, 510–514, 1995.
Kleypas, J. A., Modeled estimates of global reef habitat and carbonate production since the Last Glacial Maximum, *Paleoceanography*, *12*, 533–545, 1997.
Knox, F., and M. McElroy, Changes in atmospheric CO_2: Influence of the marine biota at high latitude, *J. Geophys. Res*., *89*, 4629–4637, 1984.
Kump, L. R., and R. B. Alley, Global chemical weathering on glacial time scales, in *Material Fluxes on the Surface of the Earth*, edited by T. M. Usselman and W. W. Hay, pp. 46–60, Natl. Res. Counc., Natl. Acad. Press, Washington, D. C., 1994.
Lea, D. W., Constraints on the alkalinity and circulation of glacial circumpolar deep water from benthic foraminiferal barium, *Global Biogeochem. Cycles*, *7*, 695–710, 1993.
Lea, D. W., and E. A. Boyle, Foraminiferal reconstruction of barium distributions in water masses of the glacial oceans, *Paleoceanography*, *5*, 719–742, 1990.
Lea, D. W., J. Bijma, H. J. Spero, and D. Archer, Implications of a carbonate ion effect on shell carbon and oxygen isotopes for glacial ocean conditions, in *Use of Proxies in Paleoceanography: Examples From the South Atlantic*, edited by G. Fischer and G. Wefer, pp. 513–522, Springer-Verlag, New York, 1999.
Ledwell, J. R., A. J. Watson, and C. S. Law, Evidence for slow mixing across the pycnocline from an open-ocean tracer release experiment, *Nature*, *364*, 701–703, 1993.
Leuenberger, M., U. Siegenthaler, and C. C. Langway, Carbon isotope composition of atmospheric CO_2 during the last ice age from an Antarctic ice core, *Nature*, *357*, 488–490, 1992.
Levitus, S., M. E. Conkright, J. L. Reid, R. G. Najjar, and A. Mantyla, Distribution of nitrate, phosphate, and silicate in the world's oceans, *Prog. Oceanogr*., *31*, 245–273, 1993.
Li, Y.-H., T. Takahashi, and W. S. Broecker, Degree of saturation of $CaCO_3$ in the oceans, *J. Geophys. Res*., *74*, 5507–5525, 1969.
Longhurst, A., *Ecological Geography of the Sea*, Academic, San Diego, Calif., 1998.
Lorius, C., J. Jouzel, C. Ritz, L. Merlivat, N. I. Barkov, Y. S. Korotkevitch, and V. M. Kotlyakov, A 150,000-year climatic record from Antarctic ice, *Nature*, *316*, 591–596, 1985.
Lynch-Stieglitz, J., and R. G. Fairbanks, A conservative tracer for glacial ocean circulation from carbon isotope and paleonutrient measurements in benthic foraminifera, *Nature*, *369*, 308–310, 1994.
Lynch-Steiglitz, J., T. F. Stocker, W. S. Broecker, and R. G. Fairbanks, The influence of air-sea exchange on the isotopic composition of oceanic carbon: Observations and modeling, *Global Biogeochem. Cycles*, *9*, 653–665, 1995.
Mahadevan, A., and D. Archer, Modeling a limited region of the ocean, *J. Comput. Phys*., *145*, 555–574, 1998.
Mahadevan, A., and D. Archer, Modeling the impact of fronts and mesoscale circulation on the nutrient supply and biogeochemistry of the upper ocean, *J. Geophys. Res*., *105*, 1209–1225, 2000.
Mahowald, N., K. E. Kohfeld, M. Hansson, Y. Balkanski, S. P. Harrison, I. C. Prentice, M. Schulz, and H. Rodhe, Dust sources and deposition during the Last Glacial Maximum and current climate: A comparison of model results with paleodata from ice cores and marine sediments, *J. Geophys. Res*., *104*, 15,895–15,916, 1999.
Maier-Reimer, E., Geochemical cycles in an ocean general circulation model: Preindustrial tracer distributions, *Global Biogeochem. Cycles*, *7*, 645–677, 1993.
Maier-Reimer, E., and R. Bacastow, Modelling of geochemical tracers in the ocean, in *Climate-Ocean Interaction*, edited by M. E. Schlesinger, pp. 233–267, Kluwer Acad., Norwell, Mass., 1990.
Maier-Reimer, E., and K. Hasselmann, Transport and storage of CO_2 in the ocean—An inorganic ocean-circulation carbon cycle model, *Clim. Dyn*., *2*, 63–90, 1987.
Maier-Reimer, E., U. Mikolajewicz, and K. Hasselmann, Mean circulation of the Hamburg LSG OGCM and its sensitivity to the thermohaline surface forcing, *J. Phys. Oceanogr*., *23*, 731–757, 1993.
Manabe, S., and A. J. Broccoli, The influence of continental ice sheets on the climate of an ice age, *J. Geophys. Res*., *90*, 2167–2190, 1985.
Margalef, R., Life-forms of phytoplankton as survival alternatives in an unstable environment, *Oceanol. Acta*, *1*, 493–509, 1978.
Marino, B. D., M. B. McElroy, R. J. Salawitch, and W. G. Spaulding, Glacial to interglacial variations in the carbon isotopic composition of atmospheric CO_2, *Nature*, *357*, 461–466, 1992.
Martin, J. H., and S. E. Fitzwater, Iron deficiency limits photoplankton growth in the northeast Pacific subarctic, *Nature*, *331*, 341–343, 1988.
Martin, J. H., G. A. Knauer, D. M. Karl, and W. M. Broenkow, VERTEX: Carbon cycling in the northeast Pacific, *Deep Sea Res*., *34*, 267–285, 1987.
Martin, J., et al., Testing the iron hypothesis in ecosystems of the equatorial Pacific Ocean, *Nature*, *371*, 123–129, 1994.
McConnaughey, T., ^{13}C and ^{18}O isotopic disequilibrium in biological carbonates, II, In vitro simulation of kinetic isotope effects, *Geochim. Cosmochim. Acta*, *53*, 163–171, 1989.
McElroy, M. B., Marine biological controls on atmospheric CO_2 and climate, *Nature*, *302*, 328–329, 1983.
McGillicuddy, D. J., and A. R. Robinson, Eddy induced nutrient supply and new production in the Sargasso Sea, *Deep Sea Res*., *Part I*, *44*, 1427–1450, 1997.
Milankovitch, M., *Mathematische Klimalehre und Astronomishe Theorie der Klimaschwankungen*, Gebrüder Borntraeger, Stuttgart, Germany, 1930.
Milliman, J. D., Production and accumulation of calcium carbonate in the ocean: Budget of a nonsteady state, *Global Biogeochem. Cycles*, *7*, 927–957, 1993.
Munk, W., and C. Wunsch, Abyssal recipes, II, Energetics of tidal and wind mixing, *Deep Sea Res*., *Part I*, *45*, 1977–2010, 1998.
Najjar, R. G., J. L. Sarmiento, and J. R. Toggweiler, Downward transport and fate of organic matter in the ocean: Simulations with a general circulation model, *Global Biogeochem. Cycles*, *6*, 45–76, 1992.
Nelson, D. M., P. Tréguer, M. A. Brzezinski, A. Laynaert, and B. Quéguiner, Production and dissolution of biogenic silica in the ocean: Revised global estimates, comparison with regional data, and relationship to biogenic sedimentation, *Global Biogeochem. Cycles*, *9*, 359–372, 1995.
Opdyke, B. N., and J. C. G. Walker, Return of the coral reef hypothesis: Basin to shelf partitioning of $CaCO_3$ and its effect on atmospheric pCO_2, *Geology*, *20*, 733–736, 1992.
Oxburgh, R., Variations in the osmium isotope composition of sea water over the past 200,000 years, *Earth Planet. Sci. Lett*., *159*, 183–191, 1998.
Peteet, D. M., J. S. Vogel, D. E. Nelson, J. R. Southon, R. J.

Nickmann, and L. E. Heusser, Younger Dryas climatic reversal in northeastern USA? AMS ages for an old problem, *Quat. Res*., *33*, 219–230, 1990.

Peterson, L. C., and W. L. Prell, Carbonate preservation and rates of climatic change: An 800-kyr record from the Indian Ocean, in *The Carbon Cycle and Atmospheric CO_2: Natural Variations Archean to Present*, *Geophys. Monogr. Ser*., vol. 32, edited by E. T. Sundquist and W. S. Broecker, pp. 251–269, AGU, Washington, D. C., 1985.

Petit, J. R., et al., Climate and atmospheric history of the past 420,000 years from the Vostok ice core, Antarctica, *Nature*, *399*, 429–436, 1999.

Rau, G. H., T. Takahashi, and M. Des, Latitudinal variations in plankton $\delta^{13}C$: Implications for CO_2 and productivity in past oceans, *Nature*, *341*, 514–516, 1989.

Rea, D. K., The paleoclimatic record provided by Eolian deposition in the deep sea: The geologic history of wind, *Rev. Geophys*., *32*, 159–195, 1994.

Redfield, A. C., The processes determining the concentrations of oxygen, phosphate, and other organic derivatives within the depths of the Atlantic Ocean, *Pap. Phys. Oceanogr. Meteorol*., *9*, 1–22, 1942.

Rhee, G.-Y., Effects of N:P atomic ratios and nitrate limitation on algal growth, cell composition, and nitrate uptake, *Limnol. Oceanogr*., *23*, 10–25, 1978.

Rind, D., and D. Peteet, Terrestrial conditions at the Last Glacial Maximum and CLIMAP sea-surface temperature estimates: Are they consistent?, *Quat. Res*., *24*, 1–22, 1985.

Rue, E. L., and K. W. Bruland, Complexation of iron(III) by natural organic ligands in the central North Pacific as determined by a new competitive ligand equilibration/absorptive cathodic stripping voltammetric method, *Mar. Chem*., *50*, 117–138, 1995.

Rue, E. L., and K. W. Bruland, The role of organic complexation on ambient iron chemistry in the equatorial Pacific Ocean and the response of a mesoscale iron addition experiment, *Limnol. Oceanogr*., *42*, 901–910, 1997.

Sanyal, A., G. Hemming, G. Hansen, and W. Broecker, Evidence for a higher pH in the glacial ocean from boron isotopes in foraminifera, *Nature*, *373*, 234–237, 1995.

Sanyal, A., N. G. Hemming, W. S. Broecker, and G. N. Hanson, Changes in pH in the eastern equatorial Pacific across the stage 5–6 boundary based on boron isotopes in foraminifera, *Global Biogeochem. Cycles*, *11*, 125–133, 1997.

Sarmiento, J. L., and R. Toggweiler, A new model for the role of the oceans in determining atmospheric pCO_2, *Nature*, *308*, 621–624, 1984.

Sarnthein, M., Sand deserts during glacial maximum and climatic optimum, *Nature*, *272*, 43–46, 1978.

Semtner, A. J., and R. M. Chervin, Ocean general circulation from a global eddy-resolving model, *J. Geophys. Res*., *97*, 5493–5550, 1992.

Shackleton, N. J., Carbon 13 in Uvigerina: Tropical rainforest history and the equatorial Pacific carbonate dissolution cycles, in *The Fate of Fossil Fuel CO_2 in the Oceans*, edited by N. R. Andersen and A. Malahoff, pp. 401–428, Plenum, New York, 1977.

Shackleton, N. J., M. A. Hall, J. Line, and C. Shuxi, Carbon isotope data in core V19-30 confirm reduced carbon dioxide concentration in the ice age atmosphere, *Nature*, *306*, 319–322, 1983.

Siegenthaler, U., and T. Wenk, Rapid atmospheric CO_2 variations and ocean circulation, *Nature*, *308*, 624–626, 1984.

Sigman, D. M., D. C. McCorkle, and W. R. Martin, The calcite lysocline as a constraint on glacial/interglacial low-latitude production changes, *Global Biogeochem. Cycles*, *12*, 409–427, 1998.

Sillen, L. G., The ocean as a chemical system, *Science*, *156*, 1189–1196, 1967.

Six, K., and E. Maier-Reimer, Effects of plankton dynamics on seasonal carbon fluxes in an ocean general circulation model, *Global Biogeochem. Cycles*, *10*, 559–583, 1996.

Sowers, T., and M. Bender, Climate records covering the last deglaciation, *Science*, *269*, 210–214, 1995.

Sowers, T., M. Bender, D. Raynaud, T. S. Korotkevich, and J. Orchardo, The $\delta^{18}O$ of atmospheric O_2 from air inclusions in the Vostok ice core: Timing of CO_2 and ice volume changes during the penultimate deglaciation, *Paleoceanography*, *6*, 679–696, 1991.

Spero, H. J., J. Bijma, D. W. Lea, and B. Bemis, Effect of seawater carbonate concentration on foraminiferal carbon and oxygen isotopes, *Nature*, *390*, 497–500, 1997.

Spero, H., J. Bijma, D. Lea, and A. Russell, Deconvolving glacial ocean carbonate chemistry from the planktonic foraminifera isotope record, in *Reconstructing Ocean History: A Window Into the Future*, edited by F. Abrantes and A. Mix, pp. 329–342, Plenum, New York, 1999.

Spitzer, W. S., and W. J. Jenkins, Rates of vertical mixing, gas exchange, and new production: Estimates from seasonal gas cycles in the upper ocean near Bermuda, *J. Mar. Res*., *47*, 169–196, 1989.

Spivack, A. J., C.-F. You, and H. J. Smith, Foraminiferal boron isotope ratios as a proxy for surface ocean pH over the past 21 Myr, *Nature*, *363*, 149–151, 1993.

Stumm, W., and J. J. Morgan, *Aquatic Chemistry*, John Wiley, New York, 1981.

Stute, M., M. Forster, H. Frischkorn, A. Serejo, J. F. Clark, P. Schlosser, W. Broecker, and G. Bonani, Cooling of tropical Brazil (5°) during the Last Glacial Maximum, *Science*, *269*, 379–383, 1995.

Sunda, W. G., and S. A. Huntsman, Iron uptake and growth limitation in oceanic and coastal phytoplankton, *Mar. Chem*., *50*, 189–206, 1995.

Sunda, W. G., D. G. Swift, and S. A. Huntsman, Low iron requirement for growth in oceanic phytoplankton, *Nature*, *351*, 55–57, 1991.

Takahashi, T., R. A. Feely, R. F. Weiss, R. H. Wanninkhof, D. W. Chipman, S. C. Sutherland, and T. T. Takahashi, Global air-sea flux of CO_2: An estimate based on measurements of sea-air pCO_2 difference, *Proc. Natl. Acad. Sci. U.S.A*., *94*, 8292–8299, 1997.

Tegen, I., A. A. Lacis, and I. Fung, The influence on climate forcing of mineral aerosols from disturbed soils, *Nature*, *380*, 419–422, 1996.

Treguer, P., D. M. Nelson, A. J. van Bennekom, D. J. DeMaster, A. Leynaert, and B. Queguiner, The silica balance in the world ocean: A reestimate, *Science*, *268*, 375–379, 1995.

Tsunogai, S., and S. Noriki, Particulate fluxes of carbonate and organic carbon in the ocean: Is the marine biological activity working as a sink of the atmospheric carbon?, *Tellus*, *Ser. B*, *43*, 256–266, 1991.

van Cappellen, P., and L. Qiu, Biogenic silica dissolution in sediments of the Southern Ocean, I, Solubility, *Deep Sea Res*., *Part II*, *44*, 1109–1128, 1997.

van Cappellen, P., and Y. Wang, Cycling of iron and manganese in surface sediments: A general theory for the coupled transport and reaction of carbon, oxygen, nitrogen, sulfur, iron and manganese, *Am. J. Sci*., *296*, 197–243, 1996.

Volk, T., and M. I. Hoffert, Ocean carbon pumps: Analysis of relative strengths and efficiencies in ocean-driven atmospheric CO_2 changes, in *The Carbon Cycle and Atmospheric CO_2: Natural Variations Archean to Present*, *Geophys. Monogr. Ser*., vol. 32, edited by E. T. Sundquist and W. S. Broecker, pp. 99–110, AGU, Washington, D. C., 1985.

Webb, R. S., D. H. Rind, S. J. Lehman, R. J. Healy, and D. Sigman, Influence of ocean heat transport on the climate of the Last Glacial Maximum, *Nature*, *385*, 695–699, 1997.

Wefer, G., G. Fischer, D. Fuetterer, and R. Gersonde, Seasonal particle flux in the Bransfield Strait, Antarctica, *Deep Sea Res*., *35*, 891–898, 1988.

Winguth, A. M. E., D. Archer, J.-C. Duplessy, E. Maier-Reimer, and U. Mikolajewicz, Sensitivity of paleonutrient tracer distributions and deep-sea circulation to glacial boundary conditions, *Paleoceanography*, *14*, 304–323, 1999.

Winguth, A., D. Archer, E. Maier-Reimer, and U. Mikolajewicz, Paleonutrient data analysis of the glacial Atlantic using an adjoint ocean general circulation model, in *Inverse Methods in Global Biogeochemical Cycles*, *Geophys. Monogr. Ser*., vol. 114, edited by P. Kasibhatla et al., pp. 171–183, AGU, Washington, D. C., 2000.

D. Archer, Department of the Geophysical Sciences, University of Chicago, 5734 South Ellis Avenue, Chicago, IL 60637. (d-archer@uchicago.edu)

D. W. Lea, Department of Geological Sciences, University of California at Santa Barbara, Santa Barbara, CA 93106-9630.

N. Mahowald, Donald Bren School of Environmental Science and Management, University of California at Santa Barbara, Santa Barbara, CA 93106. (natalie@eos.crseo.ucsb.edu)

A. Winguth, Department of Atmospheric and Oceanic Sciences, University of Wisconsin-Madison, 1225 West Dayton Street, Madison, WI 53706.